

UNIVERSITÀ DEGLI STUDI DI MILANO

SCUOLA DI DOTTORATO IN SCIENZE BIOCHIMICHE

DIPARTIMENTO DI
SCIENZE FARMACOLOGICHE E BIOMOLECOLARI

XXIX ciclo



**USE OF GENETICALLY MODIFIED MICE TO STUDY THE ANTI-
INFLAMMATORY AND IMMUNOMODULATORY ROLE OF HIGH-
DENSITY LIPOPROTEINS DURING ATHEROSCLEROSIS
DEVELOPMENT**

BIO/14

Tesi di: Giulia Sara GANZETTI

Docente guida:
Chiar.ma Prof.ssa Elisabetta GIANAZZA

Cordinatore del dottorato:
Chiar.mo Prof. Sandro SONNINO

ANNO ACCADEMICO 2016

INDEX

INTRODUCTION	1
CHOLESTEROL	2
Synthesis of cholesterol	2
Absorption of cholesterol	3
Regulation of cholesterol homeostasis	6
LIPOPROTEIN	7
Chylomicrons	9
Very low-density lipoproteins	10
Intermediate density lipoproteins	11
Low-density lipoproteins	12
High-density lipoproteins	13
<i>High-density lipoprotein structure</i>	13
<i>High-density lipoprotein metabolism</i>	13
<i>High-density lipoprotein functions</i>	14
Reverse cholesterol transport	14
Anti-inflammatory function	16
Anti-oxidative function	17
Hematopoietic function	18
Anti-thrombotic function	19
Endothelial function	20
Anti-apoptotic function	21
Anti-infectious function	22
ATHEROSCLEROSIS	22
Pathogenesis of atherosclerosis	22
<i>Inflammation in atherosclerosis</i>	24
<i>Advanced lesions in atherosclerosis</i>	26
Murine models of atherosclerosis	27
<i>EKO mouse</i>	28
<i>A-IKO mouse</i>	29
<i>LDLr/A-IKO mouse</i>	30
<i>Murine models of coronary atherosclerosis</i>	31

AIM **32**

Aim.....33

MATERIALS & METHOS **34**

Mice35
Harvesting of tissues.....35
Lipid/lipoprotein analysis36
En face analysis.....37
Histology.....37
Trasmission electronic microscopic.....38
Flow-Citometry analysis39
RNA extraction from lymphoid organs.....39
RNA-seq analysis.....40
Bioinformatic analysis.....40
Functional association analysis.....41
Statistical analysis.....41

RESULTS **42**

Plasma cholesterol profile and apoA-I concentration.....43
Atherosclerosis evaluation44
Skin phenotype46
Secondary lymphoid organs phenotype and hystology53
Leukocytes subset57
Secondary lymphoid organs transcriptomics60

DISCUSSION **62**

Discussion63

REFERENCES **69**

INTRODUCTION

CHOLESTEROL

Cholesterol is a lipid that plays several roles. This steroid, a mostly hydrophobic molecule with a 3 β -hydroxyl group, is an essential structural element of the cell membrane. Its amphipathic character allows interaction of the cholesterol polar hydroxyl group with the polar head of the phospholipids in the cell membrane, while the hydrophobic steroid ring is oriented parallel to, and buried in, the hydrocarbon chains of the phospholipid bilayer (Bastiaanse et al 1997). Thanks to these special physical properties, cholesterol reduces the fluidity (Myant 1981) and modulates the permeability, the formation of lipid raft and the functions of the proteins of the membranes (Levy et al 2007). In addition to its structural role, cholesterol is a precursor for the synthesis of steroid hormones (in surrenal glands, ovaries and testicles), bile acids (in liver) and vitamin D (in skin)(Ikonen et al 2008).

The presence of cholesterol is essential for life, but any excess entails severe clinical implications: it is thus obvious that adequate regulation of cholesterol homeostasis is necessary. Cholesterol concentration in human blood is in the range 100-300 mg/dl (Charlton-Menys et al 2008). Cholesterol homeostasis is maintained through a balance between *de novo* synthesis, intestinal absorption and fecal excretion (Wang et al 2012). The typical human diet contains 200-500 mg of cholesterol/day (Borgstrom et al 1960). Between 30 and 60% of intestinal cholesterol is absorbed through specific transporters. In addition, the steroid lipid enters the intestinal tract from other two sources: bile (800-1200 mg day) and secretion by intestinal mucosa (300 mg day). Cholesterol can also be produced *de novo* by organs as liver, intestinal wall and central nervous system. A fraction of cholesterol is continuously lost from the organism: 550 mg/day as fecal bile loss and as desquamated 250 mg/day , as unabsorbed bile salts and 100 mg/day in sebum (Levy et al 2007).

Synthesis of cholesterol

The cholesterol biosynthetic pathway (Figure 1) is a complex metabolic process that involves more than 30 reactions utilizing over 15 enzymes from many different subcellular compartments. Cholesterol is synthesized from its precursor unit acetyl coenzyme A and at least 21 steps are required to carry out the overall process. The synthesis starts with the formation of the six-carbon intermediate 3-hydroxy-3methylglutaryl-coenzyme A (HMG-CoA) from one molecule of acetyl-CoA and one of acetoacetyl-CoA, in a reaction catalyzed by the enzyme 3-hydroxy-3methylglutaryl-coenzyme A synthase (HMGCS). The enzyme 3-hydroxy-3methylglutaryl-coenzyme A reductase

(HMGCR), is bound to the membranes of the endoplasmatic reticulum and catalyzes the conversion of HMG-CoA to mevalonate. The conversion of HMG-CoA to mevalonate represents the rate limiting reaction of cholesterol synthesis. Through several condensation reactions, mevalonate is transformed into a long-chain hydrocarbon, squalene which is cyclized and transformed into cholesterol (Grundy et al 1978)(Alphonse et al 2016).

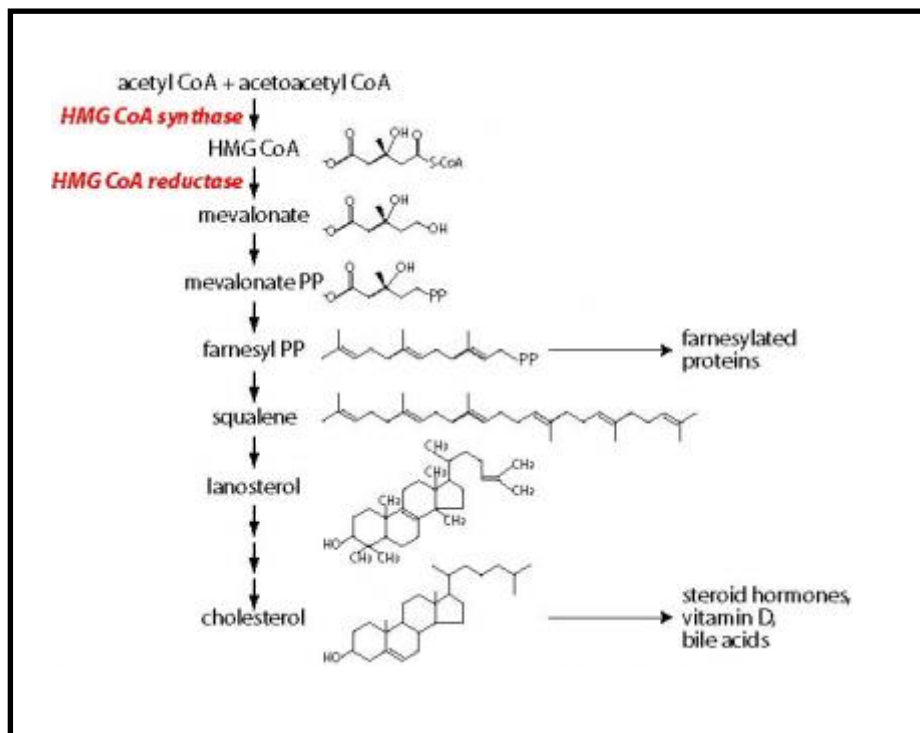


Figure 1. Pathway of cholesterol synthesis.

Absorption of cholesterol

The absorption of cholesterol (Figure 2) from the intestine is an important aspect of cholesterol metabolism. The entire small intestine can absorb this lipid from the lumen, but the major sites of absorption are in its upper part (duodenum and proximal jejunum). In addition to a simple passive diffusion through the membranes, this process involves specific proteins which are able to transport the steroid across the intestinal wall.

Niemann-Pick C1 Like 1 (NPC1L1) plays a pivotal role in cholesterol absorption. This protein, located in the proximal intestine (jejunum), actively facilitates the uptake of cholesterol by promoting the passage of sterols across the brush border membrane of the intestinal cells (Wang

et al 2007). NPC1L1 shows several of the predicted features of a plasma membrane-expressed transporter including a secretion signal, 13 putative trans-membrane domains and several potential N-linked glycosylation sites located within the extracellular loops of the protein. Moreover, this transporter contains a sterol-sensing domain, which is present in other key regulators of cholesterol homeostasis including HMGCR, SREBP cleavage-activating protein (SCAP), PATCHED, and Niemann-Pick C1 (NPC1). Studies performed on mice knock-out in this protein revealed an 80% decrease in intestinal cholesterol absorption. In addition, when NPC1L1 null-mice were treated with ezetimibe, a specific and potent inhibitor of intestinal cholesterol absorption in rodents and in humans, the treatment had no effects. Therefore, NPC1L1 represents the molecular target of ezetimibe (Altmann et al 2004).

In the proximal small intestine, NPC1L1 co-localizes with two ATP-binding cassette (ABC) transporters, ABCG5 and ABCG8, membrane proteins that transport a variety of substrates across the extra- and intra-cellular membranes. These transporters promote active efflux of un-esterified cholesterol from enterocytes into the intestinal lumen for excretion (Duan et al 2004). Intracellular cholesterol that is not effluxed by ABCG5/G8, travels to the endoplasmic reticulum (ER), where it is esterified by acyl CoA:cholesterol acyltransferase 2 (ACAT2). The esterified cholesterol is then incorporated into chylomicrons (CMs), together with triglycerides (TG), phospholipids (PH) and apolipoprotein (apo) B48 and finally it is delivered to the thoracic duct (Lee et al 2000).

Scavenger receptor type BI (SR-BI) is an additional element of intestinal cholesterol absorption. SR-BI is an 82 kDa membrane protein mostly expressed in liver and steroidogenic tissues. It is also expressed in enterocyte brush border membranes mainly at the top of intestinal villus and in the proximal part of intestine, where most cholesterol absorption occurs. However, the relevance of SR-BI in intestinal cholesterol absorption is not beyond question since the disruption of SR-BI gene in mice does not affect cholesterol absorption. The effect is thus complex with the overall process depending on the combined actions of transporter proteins involved in both uptake and efflux of cholesterol, which could compensate for the lack of SR-BI from the intestine (Hauser et al 1998).

Among the transporters facing the intestinal lumen, CD 36 seems involved in cholesterol absorption. Originally identified as a receptor for oxidized low-density lipoproteins, it is a 75–88 kDa, 472 aminoacid-long, glycosylated transmembrane protein, which actually shows a wide ligand

specificity for different lipoproteins, glycosylated proteins, thrombospondin-1 and other molecules. CD 36 is ubiquitously expressed and major sites of its synthesis are heart, skeletal muscle, adipose tissue, intestine, and the capillary endothelium (Abumrad et al 2012).

In addition, enterocytic cholesterol can be transferred to apolipoprotein A1 (apoA-I), the mainly protein component of high density lipoprotein (HDL), via ATP-binding cassette transport A1 (ABCA1) (Brunham et al 2006).

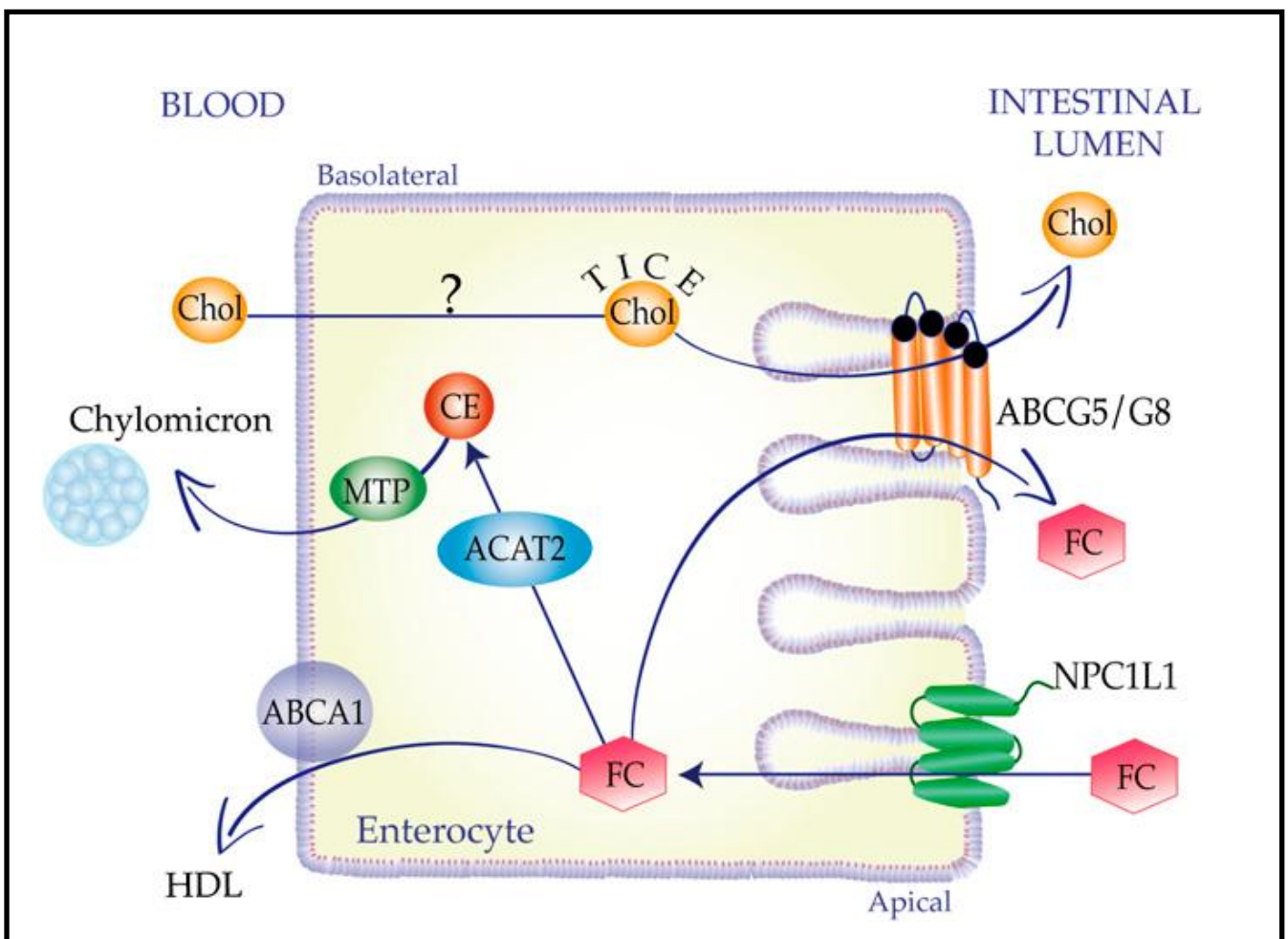


Figure 2. Pathway of cholesterol absorption.

Regulation of cholesterol homeostasis

Proper regulation of cholesterol homeostasis in the body is essential for human health. HMGCR catalyzes the conversion of HMGCoA to mevalonate, the precursor of isoprenoid groups that are incorporated into many end-products including cholesterol, ubiquinone, heme, dolichol and the farnesyl and geranylgeranyl groups that can become attached to many cellular proteins (Goldstein et al 1990). Thus, it is very important to regulate mevalonate synthesis to assure constant production of compounds that contain isoprenoid moieties. On the other hand, the synthesis of cholesterol is highly regulated also in order to prevent over accumulation and abnormal deposition in the body of toxic products, such as cholesterol itself (Kellner-Weibel et al 1998). Intracellular levels of cholesterol are tightly regulated by a system of feedback that operate at both transcriptional and post-transcriptional level (Brown et al 1997), resulting in the modulation of the expression of key proteins that control cholesterol homeostasis (Ye et al 2011).

The sterol regulatory element binding proteins (SREBPs, in particular of type 2) play an important role in this process. When cellular cholesterol is high, SREBP2 is located in the endoplasmic reticulum (ER) in a complex with SREBP2 cleavage-activating protein (SCAP). Conversely, when cells are depleted of sterols, SCAP escorts SREBP2 from the ER to the Golgi apparatus, where it is cleaved to release cleavage product from the membrane. This SREBP2 proteolytic fragment can then enter the nucleus and activate the transcription of multiple genes regulating cholesterol synthesis by binding to a sterol response element (SRE) in their enhancer/promoter regions (Horton et al 2002). SREBPs can increase the up-take of cholesterol through the activation of transcription of the LDL receptor (LDLR)(Brown et al 1997). Discovered in 1974, LDLR is a cell membrane glycoprotein involved in the binding and internalizing of circulating cholesterol containing lipoprotein particles. These endocytic receptors are ubiquitously expressed and are a key element for maintaining cholesterol homeostasis in mammals.

Liver X receptors (LXRs), a family of transcription factors that were first identified as orphan members of the nuclear receptor superfamily, play a central role in the regulation of lipid metabolism. Two isoforms exist: LXR α e LXR β . The first is expressed in spleen, liver, adipose tissue, intestine, kidney and lung, while the second is ubiquitous. The first identified target gene directly regulated by LXRs was a cytochrome P450 family member, CYP7A1, which is the rate-limiting enzyme in hepatic bile synthesis. Several studies have shown that LXRs regulate the expression of

different genes involved in cholesterol transport and metabolism. LRXs represent the key sensors of intracellular sterol levels that activate adaptive mechanism in response to cholesterol overload, including stimulation of reverse cholesterol transport and biliary cholesterol excretion, inhibition of intestinal absorption of dietary cholesterol and suppression *de novo* of cholesterol synthesis (Nakamura et al 2004). Experiments performed on mice lacking LXR α and fed a high fat diet, resulted in massive hepatic accumulation of cholesterol esters, hepatomegaly and hypercholesterolemia. This effect is due to the absence of LXR α that cannot induce CYP7A1. The only presence of LXR β in the liver cannot compensate the absence of LXR α in regulating Cyp7a1 (Peet et al 1998). In addition, LXR α is essential for the up-regulation of the ABCG5 and ABCG8 genes in response to high dietary cholesterol.

Also microRNAs (miRNAs), members of a class of non-coding RNAs, are considered novel post-transcriptional regulators of cholesterol homeostasis (Meaney et al 2014). In particular, microRNA-33 (miR-33) can down regulate the expression of ABCA1 and ABCG1, resulting in the control of cholesterol efflux and HDL biogenesis. Other miRNAs, such as miR-122, miR-370, miR-378-378, miR-125a, miR-27 and miR355, are involved in cholesterol homeostasis (Goedeke et al 2012).

LIPOPROTEINS

As completely insoluble in water, cholesterol cannot circulate freely in plasma but must be transported by complex carriers: the lipoproteins (Grundy et al 1978). Lipoproteins are macromolecules containing an hydrophobic central core of neutral lipids such as cholesteryl esters (CE) and triglycerides and a surface rich in proteins (apolipoproteins), and in polar lipids, mainly phospholipids and unsterified (free) cholesterol (FC)(Figure 3)(Rader, D. J 2008).

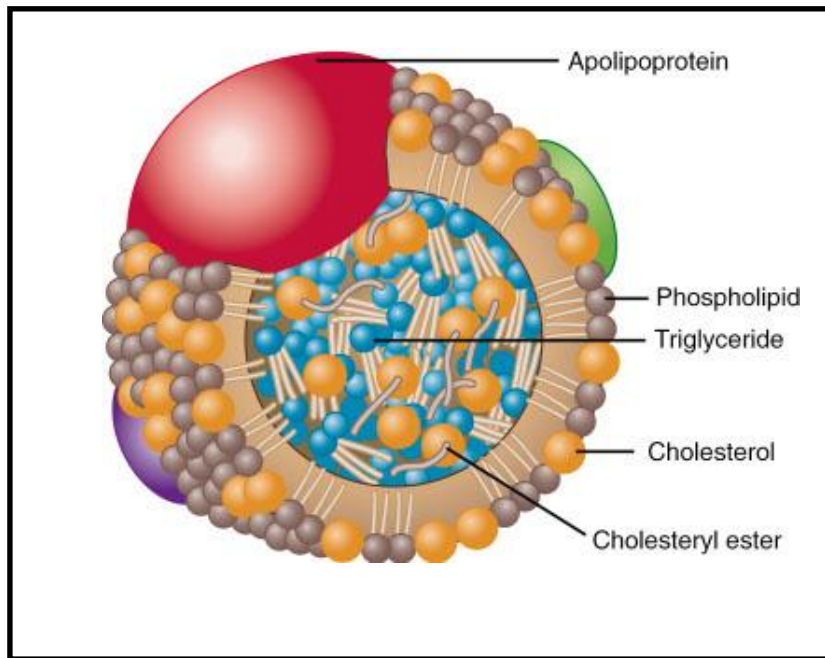


Figure 3. Representation of lipoprotein structure.

Plasma lipoproteins are characterized by a different ratio between free cholesterol (FC), esterified cholesterol (CE), PL, TG and by the presence of different apolipoproteins. They are classified into five major classes: chylomicrons, very low-density lipoprotein (VLDLs), intermediate-density lipoprotein (IDLs), low-density lipoprotein (LDLs) and high-density lipoprotein (HDLs)(Table 1) (Hoofnagle et al 2009).

Lipoprotein class	Density (g mL ⁻¹)	Diameter (nm)	% Protein	% Cholesterol	% Phospholipid	% Triglycerides
HDL	1.063–1.210	5–15	33	30	29	8
LDL	1.019–1.063	18–28	25	50	21	4
IDL	1.006–1.019	25–50	18	29	22	31
VLDL	0.95–1.006	30–80	10	22	18	50
Chylomicrons	<0.95	100–1000	<2	8	7	84

Table 1. Classification and properties of plasma lipoproteins.

Chylomicrons

Chylomicrons are the largest lipoproteins (up to 100 mm in diameter) with the lowest protein-to-lipid ratio (being about 90 percent lipid) and therefore they are the least dense (less than 0.95 g/ml). CMs are triglyceride-rich particles with a central lipid core and an outer layer of phospholipids, free cholesterol and apolipoproteins (Hamilton R.L. 1972). ApoB48 represents the main apolipoprotein in this particles, but other apolipoproteins are on their surface, including apoA1, apoAIV, and apoCs (Hussain et al 1996). CMs are formed in enterocytes in response to fat ingestion; they transport dietary triglycerides to peripheral tissues and cholesterol to the liver (Julve et al 2016). Triglycerides, which represent the principal fat in diet, are absorbed from mixed micelles formed in the intestinal lumen by fatty acids and monoglycerides after the hydrolysis of the ester bonds catalyzed by intestinal and pancreatic lipases. In the endoplasmic reticulum of enterocytes, triglycerides are resynthesized and complexed with ApoB48, in a process involving Microsomal Triglyceride Transfer Protein (MTP), to form primordial chylomicrons particles (pre-chylomicron)(Olofsson et al 2000). Then, the pre-chylomicrons are included in a unique transport vesicle, the pre-chylomicron transport vesicle (PCTV), which are budded off the endoplasmic reticulum (ER) membrane and transported to the Golgi apparatus (Kumar et al 1999). Once into the Golgi compartment chylomicrons undergo further modifications such as addition of apoA-I and glycosylation of apoB48. They are then fused

into another transport vesicle and are transferred to the basolateral membrane for secretion in the general circulation (Hussain et al 2000).

Once chylomicrons are secreted via the intestinal lymphatic system they enter the blood circulation, bind some apoE and ApoC and eventually come into contact with lipoprotein lipase (LPL), which is located on the luminal surface of the vascular endothelium of tissues such as skeletal muscle and adipose tissue. This enzymes, activated by apoC-II, hydrolyses the triglycerides of CM, which as a result become smaller, cholesterol-rich chylomicron remnants. The released fatty acids and monoglycerides are either taken up locally by cells, in which they are used for energy or stored as triglycerides in adipocytes (Cooper et al 1997). Remnants are cleared from the circulation by the liver in a process that involves apoE, present on the chylomicron remnants, apoE binds to the LDL receptor and to other hepatic receptors such as LDL receptor like protein (LRP) leading to the up take of the entire particle by the hepatocytes (Mjos et al 1975). Remnants contain apoB48 as their nascent precursors, but have different composition and structure from CMs. They are depleted in tryglicerides, phospholipids and apoCs and are enriched in cholesteryl esters (CE), which they acquire from HDL through the action of cholesteryl ester transfer protein (CETP).

Very Low-Density Lipoproteins

Very low-density lipoproteins (VLDLs) are characterized by a density between 0,95 and 1006 g/ml and by a diameter of 30-80 nm. As CMs, VLDLs are triglyceride-rich lipoproteins containing small amounts of cholesterol and phospholipids. They represent the major vehicle in the plasma which transfer triglycerides synthetized in the liver to peripheral tissues. Thus, CMs transport dietary lipids, whereas VLDLs are involved in endogenous lipid pathway. VLDLs are produced by the liver, where triglycerides and cholesterol esters are transferred to ER with Apo B-100, a large hydrophobic protein which represents the main structural component of these lipoproteins. As for CMs, the assembly of triglycerides and the apoB-100 to form VLDLs is mediated by MTP. After their biogenesis, in the ER, VLDLs are transferred by a specialized transport vesicle, the VLDL transport vesicle, into the Golgi apparatus, for their eventual secretion from the hepatocytes (Tiwari et al 2012). The availability of triglycerides is the main determinant of the rate of VLDLs synthesis. MTP is essential for the association between lipid and Apo B-100. Mutations of MTP result in the failure block of VLDLs production and in a marked decrease in plasma levels of

triglycerides and cholesterol. Betaipoproteinemia is caused by molecular defect in this process. If either the supply of triglycerides is limited or MTP is altered, the newly synthesized Apo B is rapidly degraded. When VLDL particles are secreted into the circulatory system, the triglycerides are hydrolyzed by LPL, fatty acids are released and the particles acquire apoE and apoC from HDL. This change leads to the formation of IDLs (Shelness et al 2001).

Intermediate density lipoproteins

IDL particles have an intermediate density of 1,006-1,019 g/ml and a diameter of 25-30 nm. These lipoproteins are relatively enriched in cholesterol esters, contain apoB-100 and acquire Apo E from HDL particles. IDLs are present in blood at low concentration and are characterized by a short half-life. As the remnants, IDL particles are removed from the circulation by the liver via the LDL receptors. While remnants are rapidly removed from the blood by the liver, only a fraction of IDL particles are cleared. The triglycerides remaining in the IDL are hydrolyzed by the hepatic lipase. This event leads to an additional decrease in triglyceride content and the exchangeable apolipoproteins are transferred from the IDL particles to other lipoproteins to form LDL (Tatami et al 1981).

Low density lipoprotein

LDLs are lipoproteins with density of 1,009-1063 mg/dl and whit size of 18-28 nm. These particles are the major carriers of circulating cholesterol and represent the final stage of catabolism of VLDL, through the progressive depletion in triglycerides content (Figure 4). LDLs are formed by a core of cholesterol esters surrounded by a phospholipid monolayer and apoB-100, that in addition to its structural function, it behaves as a ligand (Driscoll et al 1986). The main function of LDL particles is to transport and deliver cholesterol to peripheral tissues. The LDL lipoproteins are removed via whole-particle endocytosis mediated by LDLR (Goldstein et al 1985). These receptors are expressed mainly on hepatocytes surface. The receptor-LDL complex, is internalized as a part of a vesicle; the LDL particles are then released inside a lysosome, a cellular organelle that contains acid hydrolases that could easily digest all the components of LDL and free cholesterol. LDL lipoproteins concentration in plasma is determined by the rate of LDL production and clearance. Both processes are regulated by the number of LDLR in the liver. An increase in hepatic LDLR leads to increase LDL clearance resulting in reduction of plasma LDL levels. On the other

hand, a decrease in hepatic LDLR slows LDL clearance leading to an increase in plasma LDL levels. The expression of these receptors is subjected to feedback regulation by the cholesterol content of the cells. When the intracellular cholesterol increases, the synthesis of LDLR is reduced, so the uptake of LDL by the cell is reduced. Conversely, when cell cholesterol levels decrease, SREBPs, which are transcription factors that modulate the expression of LDLR, together with other gene products involved in cholesterol metabolism, are transported to the nucleus, where they stimulate the transcription of their targets. As previously mentioned, this include HMG-CoA reductase, the regulatory enzyme of cholesterol synthesis (Goldstein et al 2009).

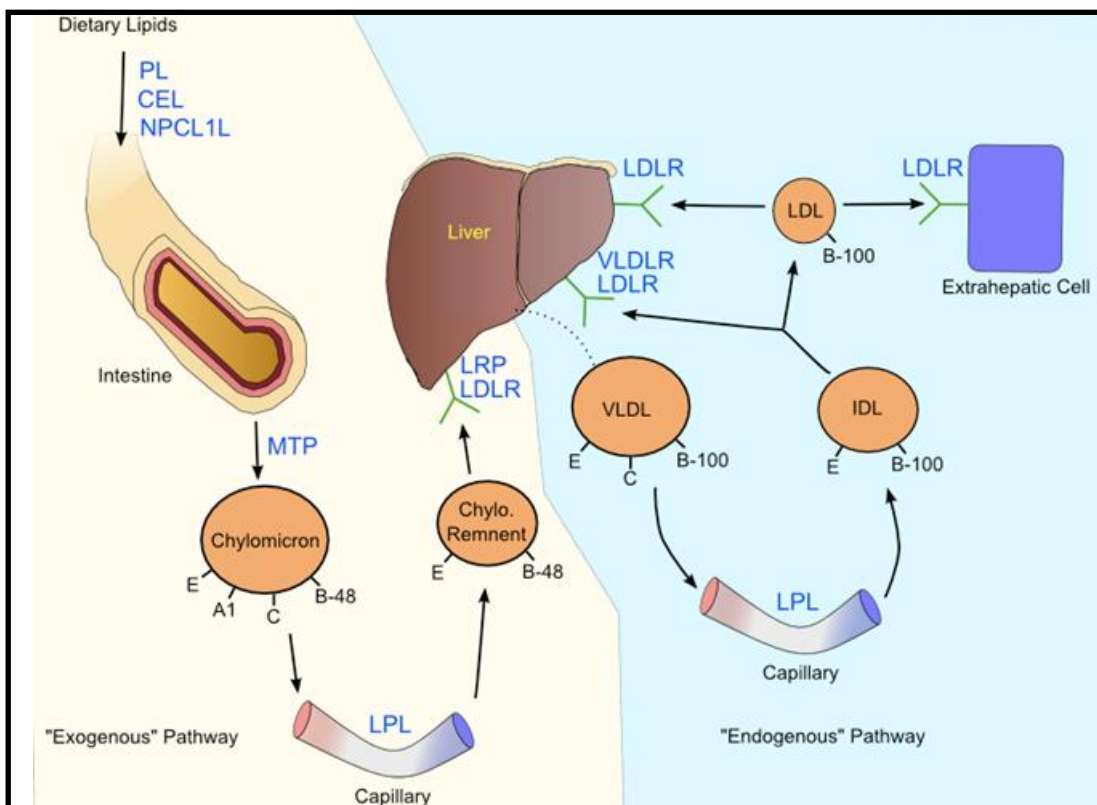


Figure 4. Metabolism of VLDL and LDL lipoproteins.

High density lipoproteins

High-density lipoproteins structure

HDLs are lipoproteins characterized by a density of 1.063-1.210 g/ml and by a diameter of 5-15 nm. HDLs are dynamic particles and represent an heterogeneous family of lipoproteins differing in size, shape, charge and density. HDL are constituted by 50% protein and 50% lipid. Most part of plasma HDLs are characterized by globular shape, with a core of neutral lipids (triglycerides and cholesteryl esters) stabilized by a surface of polar lipids (phospholipids and unsterified cholesterol) and apolipoproteins (Gu et al 2010). HDL particles are heterogeneous in their proteome. The protein component of HDL is formed principally by apoA-I (70%) and apoA-II (20%). Recent proteomic analysis have identified more than 60 proteins among them other apolipoproteins such as apoA-IV, apoCs, apoE, as well as many enzymes including lecithin:cholesterol acyltransferase (LCAT), cholesteryl ester transfer protein (CEPT), phospholipid transfer protein (PLTP) and paraoxonase (PON) (Shah et al 2013).

HDL can be classify on the basis of density, charge, shape and size. Based on density, it is possible to identify two different HDL subclasses, called HDL2 (1.063 to 1.12 g/ml) and HDL3 (1.12 to 1.21 g/ml). As for charge, it was discovered that, upon agarose gel electrophoresis, HDL split into α - and pre- β -migrating particles. By combining charge and size these two subclasses can be categorized into 12 distinct apoA-I-containing HDL particles, referred to as pre- β (pre- β 1 and pre- β 2), α (α 1, α 2 and α 3) and pre- α (pre- α 1, pre- α 2 and pre- α 3) on the basis of whether their mobility is slower or faster, respectively, than that of albumin and of whether their size is larger or smaller. Finally five different subclasses were identified on the basis of particle size: HDL3c, 7.2-7.8 nm; HDL3b, 7.8-8.2 nm; HDL3a, 8.2-8.8nm; HDL2a, 8.8.-9.7 nm; HDL2b, 9.7-12.0 nm (Nichols et al 1986).

High-density lipoprotein metabolism

HDL lipoproteins are synthesized by liver and intestine and part of them delivers from triglyceride-rich lipoproteins. The newly-made HDLs, so called “nascent HDLs”, have a discoidal shape. These HDL particles are essentially composed of PL and apoA-I (Duong PT 2008). Once in the circulatory system they participate in reverse cholesterol transport, a process that removes the excess of

cholesterol from peripheral tissues and delivers it to liver (Miller 1990). Nascent HDLs represent a substrate for lecithin:cholesterol acyltransferase (LCAT), a 63-KDa glycoprotein primarily synthesized in the liver and a lower extent in other tissues, such as brain and testes, that esterifies the free cholesterol of HDLs into cholesteryl ester. The hydrophobic nature of CE allows its to transfer into core of HDL particles, which results in a spherical shape for cholesterol-laden HDLs. Only a trace amount of CE remains in the core of HDL. CETP, an enzyme present in human, but not in mice, mediates the equimolar transfer of the majority CE from HDLs for TG from LDLs, VLDLs or chylomicrons. Triglycerides on HDL lipoproteins are catabolized by hepatic lipase leading to the formation of small HDL particles. The cholesterol on HDLs is above all delivered to the liver, through a transport mediated by SR-B1. After this step, the cholesterol-depleted HDLs become smaller in size and go back to circulatory system.

High-density lipoprotein functions

Several studies have showed the existence of a strong correlation between plasma high-density lipoprotein cholesterol levels and the incidence of vascular disease (Gordon et al 1977). The athero-protection mediated by HDL is exerted through reverse cholesterol transport (RTC), as well as through their anti-oxidant, anti-apoptotic, anti-inflammatory and anti-thrombotic properties.

Reverse Cholesterol Transport

The anti-atherogenic action of HDLs is mainly due to the reverse cholesterol transport (RCT) (Figure 5), a pathway that removed cholesterol from peripheral cells, including macrophages within the arterial wall, and delivers it to the liver for excretion through bile and feces. With this process, HDL particles decrease cholesterol accumulation in vessel walls, preventing atherosclerosis development (Franceschini et al 1991). RCT is a complex process in which the HDLs and their mainly protein component ApoA-I play a key role.

Cholesterol efflux from cells of peripheral tissues represents the first and limiting step of RCT. Several *in vitro* studies have shown the ability of HDL particles to promote the removal of cholesterol from cell membranes (von Eckardstein et al 1996). ApoA-I plays a key role in this process, through its interactions with the surface of plasma membranes and with the receptors involved in efflux. Cholesterol can be removed by HDL via a number of mechanisms. The first one

is aqueous diffusion, the passive diffusion of cholesterol from plasma membranes to HDLs, which occurs according to the direction of cholesterol gradient (Rothblat et al 1992). The second is receptor-mediated process. Different membrane proteins have been identified as players in this pathway. Among them, ATP-binding cassette transporter A1 (ABCA1) is involved in an unidirectional (cell to acceptor) and ATP-dependent transport. Lipid-free/lipid-poor apolipoproteins, in particular apoA-I, represent the principal cholesterol ABCA1 acceptors (Jessup et al 2006). The interaction between ABCA1 and apoA-I promotes cholesterol and phospholipid efflux from ABCA1 to apoA-I, with generation of small, discoidal pre- β -HDL. These particles can remove further cholesterol from cells through the same pathway (Favari et al 2009). Mutations in the ABCA1 gene, results in Tangier Disease, an autosomal recessive disorders characterized by an almost totally absence of HDL-cholesterol, by reduced LDL-cholesterol, by high levels of triglycerides and by cholesterol accumulation in several tissues such as liver, spleen and intestine. The patients affected by Tangier Disease are unable to produce discoidal HDL hence cannot promote peripheral cholesterol removal (Brooks-Wilson A 1999). A second transporter, ATP-binding cassette transport G1 (ABCG1), is involved in cholesterol homeostasis. Also this receptor is characterized by unidirectional ATP-dependent transport. ABCG1 is an essential cholesterol acceptor for all plasma HDL subclasses, including mature α -HDL particles and discoidal pre- β -HDL. The pivotal role in HDL-mediated cholesterol efflux by both ABCA1 and ABCG1 is suggested by their high expression in macrophages, in particular after cholesterol loading. SR-BI mediates bidirectional flux of unesterified cholesterol between cells and mature HDLs, but not small pre- β -HDL (Jessup et al 2006). SR-BI is active not only in the first step of RCT, but also in the last phase during the up-take of mature HDLs by liver.

The free cholesterol accumulated in pre- β -HDLs is solubilized in the phospholipid layer at the surface of HDL particles to be rapidly esterified by LCAT with the formation of cholesteryl esters. Being an activator of LCAT, apoA-I represents a key of esterification. The hydrophobic CE is then moved to the core of HDLs whereas free cholesterol is removed from the surface of the HDL, leading to an expansion of these lipoproteins to become spherical HDLs.

Once CEs are accumulated in their core HDLs transport CE to peripheral cells and tissues, and back to the liver through different mechanisms. CETP can catalyzed the transfer of cholesteryl ester, generated by LCAT, in HDLs to apoB containing lipoproteins laden with triglycerides. The resulting

lipoproteins characterized by a low density are then catabolized by the liver. The lipid-free and lipid-poor apoA-I, which dissociates from HDL particles as a consequence of CETP-mediated transfer of core lipids to other lipoproteins, may be cleared from the circulation by the endocytic receptors, megalin and cubulin, which are expressed in the kidney (von Eckardstein et al 2001). Cholesteryl esters are also selectively removed from HDLs when they bind to SR-BI on the surface of hepatocytes (Glass et al 1983). *In vitro* studies have demonstrated that the hepatic lipase facilitates this process through a mechanism that involves the binding of HDLs to the cell surface. (Lambert et al 1999). Furthermore, HDLs can accumulate apoE and are eventually taken up by liver through the LDL receptors.

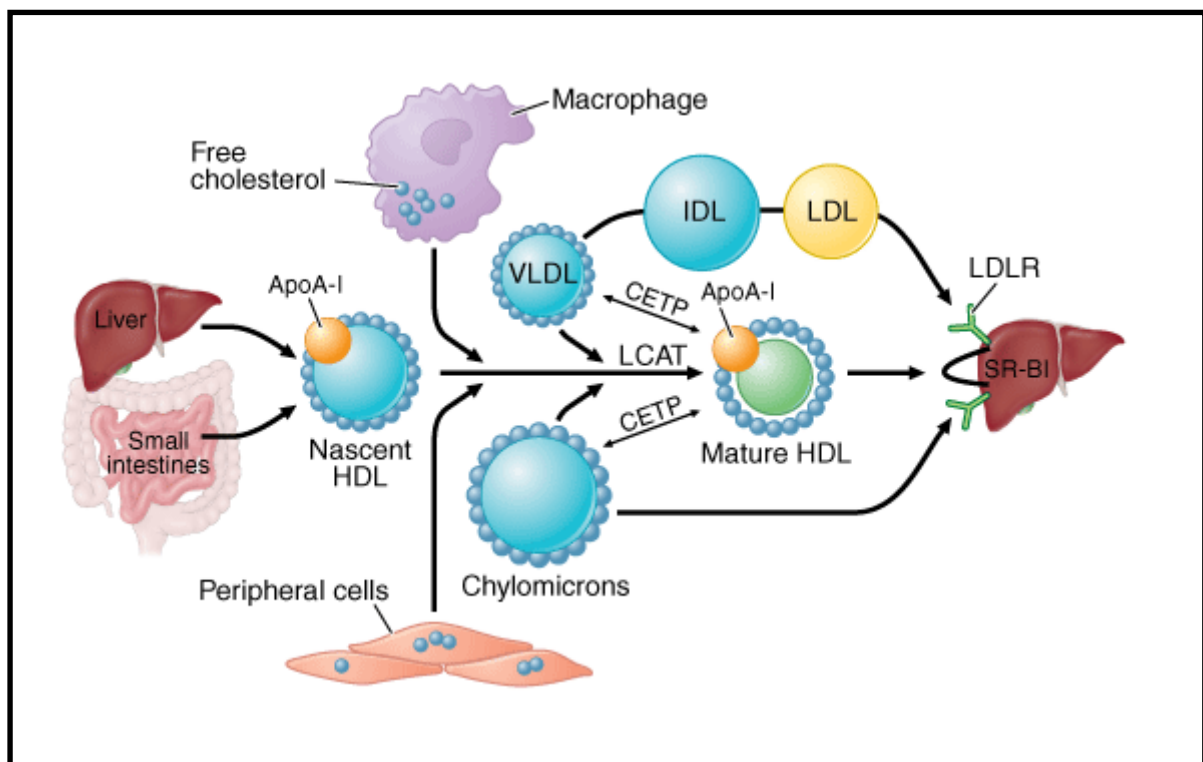


Figure 5. Pathway of reverse cholesterol transport

Anti-inflammatory function

Among the anti-atherogenic functions of HDLs in addition to RCT, one of the best studied is the anti-inflammatory properties. HDLs have been known for 20 years to be anti-inflammatory particles (Cockerill GW 1995). Atherosclerosis is a chronic inflammatory disease characterized by

accumulation of oxidized LDLs (LDL-ox) and by the presence in the vessel walls of inflammatory cells such as macrophages, differentiated from monocytes, and T lymphocytes and by plasma several inflammatory markers (Libby 2002). LDL-ox stimulate endothelial cells to express monocyte chemoattractant protein-1 (MCP-1). The production of this factor promotes the migration of leukocytes into the arterial vessel. HDL particles are able to suppress the expression of MCP-1, decreasing monocytes transmigration (Navab M 1991). When monocytes enter the arteries, LDLox induce their differentiation into macrophage, the most important inflammatory cell of atherosclerosis. Through cytokines production, these cells are able to activate endothelial cells, in which they induce the expression of cell adhesion molecules including vascular cell adhesion molecule-1 (VCAM-1), intercellular adhesion molecule-1 (ICAM-1) and E-selectin (Baker PW 1999). The induction of these adhesion proteins is mediated by NF- κ B transcriptional activation. HDLs can exert the anti-inflammatory properties inhibiting endothelial cell and monocytes activation through the suppression of NF- κ B activity; the latter is made possible by inhibition of sphingosine kinase, an enzyme involved in a key steps of the synthesis of the adhesion proteins (Xia et al 1999). Synthetic HDLs, obtained through the association between phosphatidylcholine and apoA-I, exert an inhibition on this cytokine-induced expression (Calabresi L 1997). Another anti-inflammatory effect of HDLs involves the transport of sphingosine-1-phosphate (S1P) a lipid mediator endowed anti-inflammatory properties at low concentration (Sato et al 2010).

Anti-oxidative function

LDL particles represent a major risk factor in atherogenesis after undergoing oxidative modifications (Steinberg 1997). The oxidation process induces several structural and compositional alteration in apoB. The presence of oxidized LDL and their accumulation in vessel wall play a pivotal role both in early and in late stages of atherogenesis. Ox-LDL and oxidized lipids can induce pro-inflammatory phenotypes which lead to endothelial dysfunction and apoptotic cell death, key steps in the initiation and progression of the atherosclerotic plaques (Navab et al 2011). HDL particles are heterogeneous in their capacity to protect LDL against oxidative modification (Bandeali et al 2012). HDL particles prevents LDL from free radical-induced oxidative damage through several mechanisms. The antioxidant effect is attributed to the capacity of HDLs to chelate transition metal, to extract lipids peroxidation products from oxidized lipoproteins or cellular membranes, to accept phospholipid-containing hydroperoxides from oxidized membranes

and to promote the transfer of hydroperoxides and other lipid peroxidation products from ox-LDL (Navab et al 2001). HDL particles contain several antioxidant enzymes that can be involved in the degradation of lipid hydroperoxides such as paraoxonase-1 (PON1), LCAT, platelet-activating factor acetylhydrolase (PSF-AH) and lipoprotein-associated phospholipase A2 (Lp-PLA2). These enzymes may either directly prevent LDL oxidation or degrade oxidized bioactive products in LDLs. In particular, the most prominent anti-oxidative capacity is associated with PON1, an enzyme located only on HDL and synthesized by the liver. Over-expression of PON1 in mice confers enhanced HDL anti-oxidative capacity, and PON1 itself prevents LDL oxidation *in vitro* (Tward A 2002). Most importantly, HDLs isolated from mice lacking PON1 have reduced ability to prevent LDL oxidation. However it is very difficult to separate PON1 from other HDL components. ApoA-I itself exerts anti-oxidant effects. It plays an important role in the maintenance of the lipid environment in which enzymes such as PON1 and lecithin: cholesterol acyl transferase (LCAT) can operate. ApoA-I is essential in accepting oxidized lipids from ox-LDL as well as from cells and in creating a safe environment for the release of lysophospholipids and their subsequent transfer to the liver (Garner B 1998). Cell culture experiments showed that apoA-I is able to remove lipids from LDL and thereby to make LDL resistant to vascular cell-mediated oxidation and to prevent oxidized LDL-induced monocyte adherence and chemotaxis (Navab et al 2000).

Hematopoietic function

HDL particles play an important role in hematopoiesis. Several studies performed on ABCA1^{-/-};ABCG1^{-/-} mice showed that a deficit in cholesterol efflux transporters leads to leukocytosis, which is associated with atherosclerosis pathogenesis (Out et al 2008). In this model, fed a standard chow diet, an increase of myeloid cells, monocytosis, neutrophilia and eosinophilia were observed. When these animals were fed a high-fat diet, peripheral leucocytes and monocytes increased further. These results suggest a pivotal role for these transporters in the maintenance of myeloid cell homeostasis. Both ABCA1 and ABCG1 are expressed in hematopoietic stem and multipotential progenitor cells (HSPCs). A deficit in these transporters leads to an increase in the number of HSPCs. HDL particles are able to reverse the hyperproliferation of HSPCs in the absence of ABC transporters by promoting cholesterol efflux through passive aqueous cholesterol diffusion or other mechanisms.

ApoA-I is not expressed in hematopoietic stem cells and the apoA-I deficit in murine models does not lead to monocytosis and HSPCs ((Yvan-Charvet et al 2010)). The study performed on Ldlr-/-apoA-I-/- mice fed high fat diet, showed an enlargement of lymph nodes and spleens in comparison with Ldlr-/- (Wilhelm et al 2009). This result suggests that apoA-I exerts a pivotal role in the regulation of peripheral lymphocyte proliferation in hypercholesterolemia. In particular, the deletion of apoA-I lead to an increase of cholesterol in lymph nodes as well as to the expansion of all classes of lymph nodes cells with a significant increase in T cell proliferation and activation. When Ldlr-/-apoA-I-/- mice were treated with apoA-I injections, the number of LN immune cells decrease. ApoA-I treatment increased T regulatory cells while decreasing the percentage of effector T cells. These results suggest that apoA-I is involved in control of T cell homeostasis in peripheral lymphoid organs through the modulation of the balance among T cells (Wilhelm et al 2010). The ability of HDL and of their main protein component apoA-I to suppress monocytosis, neutrophilia, monocyte and T-cell activation, stem cell mobilization and extra-medullary hematopoiesis appear to represent the key anti-atherogenic properties.

Anti-thrombotic function

Vascular endothelium damage leads to platelets and coagulation factors activation. The main role of platelets is to seal the damaged vessel wall upon injury and to promote repair of the endothelium via the release of cytokines, chemokines, and growth factors (Broos et al 2011). Excessive platelet aggregation or activation causes thrombus formation. Dysfunction of endothelium can modify hamper its ability to participate in control of coagulation and fibrinolysis. LDL and ox-LDL, the pro-atherogenic lipoproteins are responsible for the increased susceptibility to thrombosis (Rosenson et al 1998). Conversely, HDL particles display anticoagulant effects (Griffin et al 2001). HDL particles can affect both count and characteristics of platelets and modulate the risk of atherothrombosis events via the megakaryocyte- platelet hemostatic axis (Martin et al 2012). Dyslipidemia does change the characteristics of megakaryocytes, which represent the precursor cells residing in the bone marrow. Several studies performed both in animal models and in humans, have shown that in hypercholesterolemia the megakaryocytes are significantly larger and have a higher mean ploidy in comparison with control condition (Pathansali et al 2001). High ploidy megakaryocytes generates larger and more active platelets (Corash et al 1987). HDLs exert an inhibitory effect on platelet functionality through their action on platelets and on endothelial cells. HDL particles inhibit platelet aggregation caused by both ADP and thrombina (Nofer et al

1996). Platelet aggregation is inversely correlated with HDL-C levels and with the extent of thrombosis (Naqvi TZ 1999). The infusion of a mutant form of apoA-I, apoA-IMilano in rats and the administration to humans of rHDL that contain it result in the inhibition of platelet activation (Li D 1999; Calkin AC 2009).

In addition to their anti-aggregation activity, HDL particles also display anticoagulant effects, through the suppression of the coagulation cascade. The final step of this cascade is characterized by the conversion of prothrombin into thrombin, in the presence of factors X_a and V_a and of Ca^{2+} . This conversion occurs on the surface of membranes that contains anionic phospholipids. HDLs have the ability to inhibit this conversion, blocking the transbilayer diffusion of anionic lipids, essential for the formation of the procoagulant complex (Epanand et al 1994). Phosphatidylinositol 4,5-bisphosphate plays a pivotal role in this process. Several complement system factors are able to activate the coagulation cascade and HDL particles have demonstrated an inhibitory activity also at this level (Sulpice et al 1994).

Endothelial function

The endothelium significantly contributes to maintain vascular tone through the production of several substances. Among them, nitric oxide (NO) and prostacyclin (PGI₂) play a central role. A decrease in their availability leads to endothelial dysfunction; several studies have shown that HDLs induce the increase of NO and PGI₂ production both with direct and indirect mechanisms (Calabresi et al 2003). Studies performed on endothelial cells, demonstrated that HDL particles increase the abundance of endothelial NO synthase (eNOS) protein through both transcriptional and posttranslational modulation, prevent eNOS displacement from caveolae and promote the activation of eNOS (Kuvin et al 2002). eNOS activation involves HDL binding to SR-BI, which activates the phosphatidylinositol-3-kinase (PI3K)/Akt signalling pathway and the phosphorylation of endothelial nitric oxide synthase (eNOS) (Besler et al 2011). In addition, HDL can mediate eNOS activation through the interaction of sphingosine-1-phosphate (S1P) with its receptors. S1P is a bioactive phospholipid associated with HDL, in which it is specifically bound to apolipoprotein M (apoM), which thus represents a vasculo protective constituent of HDL (Christoffersen et al 2001). Cultured endothelial cell experiments demonstrated that HDLs increase PGI₂ through different

mechanisms. HDL can supply endothelial cells with arachidonate, that is a substrate for PGI₂ synthesis (Pomerantz et al 1985), or can activate a calcium-sensitive (Tamagaki et al 1996), membrane-bound phospholipase that makes endogenous arachidonate available for PGI₂ synthesis (Van Sickle et al 1986). *In vivo* experiments support the relevance of HDL in promoting endothelium dependent vasodilatation. Studies performed on hypercholesterolemic apoE-deficient mice demonstrated that intravenous injections of synthetic HDL (sHDL) restore endothelium dependent dilation with a dose-dependent effect (Kaul et al 2004). In humans, plasma HDL-C concentration is a strong independent predictor of NO dependent peripheral vasodilation in healthy individuals as well as in hyperlipidemic, diabetic and coronary patients (Zhang et al 2000). The intravenous infusion of sHDL in subjects with hypercholesterolemia or with low HDL-C rapidly restores the altered endothelium dependent peripheral vasodilation through increased NO bioavailability (Spieker et al 2002).

Anti-apoptotic function

Cell apoptosis in response to endothelial damage represents a pivotal feature in atherosclerosis and other vascular diseases. HDL particles exert several anti-apoptotic properties that increase cell survival. Growth factor deprivation-related apoptosis of cells is inhibited by HDL. These lipoproteins support mitochondrial function, reduce reactive oxygen species, prevent the release of apoptotic signals, such as cytochrome C and suppress the activation of caspase 3 and caspase 9, a family of protease involved in programmed cell death (Suc et al 1997). By activating PI3K/Akt, HDLs drive the expression of endothelial antiapoptotic Bcl-xl, and suppresses Bid, a pro-apoptotic protein. HDL mediates changes in the expression of genes through cell signaling and via NO production and through activation of surface receptors by the action of HDL-associated proteins and of bioactive lipids, including apolipoprotein J (apoJ) and S1P (Riwanto M 2013). It is likely that alternative anti-apoptotic mechanisms resulting from HDL-induced signaling are also at work. Overall, HDL has been demonstrated to suppress apoptosis in endothelial cells. Different proatherogenic factors such as tumor necrosis factor (TNF α) and oxLDL, can promote endothelial cell apoptosis, causing an increase of intracellular calcium that lead to cell death. This process is reversed by HDL, which prevent calcium increase (Suc et al 1997). HDL-associated lysophospholipids sphingosylphosphorylcholine and lysosulfatide protect endothelial cells from the effects of growth factors related to apoptosis, both by blocking the mitochondrial pathway of

apoptosis and by activating Akt. Moreover, lysophospholipid sphingosine-1-phosphate (S1P) increase cell survival (Nofer et al 2001). HDL promotes vascular cell migration, proliferation, survival and recruitment of endothelial progenitor cells (EPCs) to sites of vascular injury (Di Angelantonio et al 2009).

Anti-infectious function

HDL particles are involved also in innate immunity by their ability to modulate immune cell function. A large number of studies have demonstrated that lipoproteins act as anti-infectious, anti-parasitic, and anti-viral agents by binding microorganisms or compounds derived from microorganisms. When either lipopolysaccharides (LPS), from gram negative bacteria, or lipoteichoic acid (LTA), from gram positive bacteria, are incubated with whole blood from healthy humans, the majority of the LPS and LTA are bound to HDL. This interaction with HDL prevents LPS and LTA interaction with toll-like receptors (TLR) and the resulting activation of macrophages (Khovidhunkit et al 2004). TLR activation of macrophages stimulates the production and secretion of cytokines and other signaling molecules, which if produced in excess can lead to septic shock and to death (Beutler et al 2003). Some studies have shown that HDLs, in addition to binding LPS, also facilitates the release of LPS that is already bound to macrophages, reducing macrophage activation. The capacity of LPS neutralization is related to both the lipid and protein components of HDLs. HDLs have also protective properties from parasitic infections. In addition, HDLs binds a wide variety of viruses and neutralizes their activity. HDL particles are able to kills Trypanosome brucei brucei and Trypanosome brucei rhodesiense, parasites that cause sleeping sickness, by creating ionic pores in endosomes. This effect is made possible when apolipoprotein L1 (apo-L1) (also known as trypanosome lytic factor) is present in specific sub-classes of HDL (Hajduk SL 1989).

ATHEROSCLEROSIS

Pathogenesis of Atherosclerosis

Cardiovascular disease (CVD) is the main cause of death in worldwide; coronary disease, namely heart attacks and stroke, kills 4500 people every day in Europe and more than 17 million people in the world (WHO 2011). Atherosclerosis is a complex multifactorial chronic disease with different etiologies that synergistically promote lesion development (Figure 6) (Roger et al 2012). Among

them, elevated plasma concentration of cholesterol, especially LDL-Cs, genetic predisposition, age, gender, smoking, hypertension, stress, poor dietary habits and physical inactivity, represent the major risk factors. The first step in atherosclerosis development is a damage to, or thickening of, endothelium, a permeable barrier between blood and tissues. Endothelial injury of arterial walls occurs mainly in large and medium arteries, characterized by the presence of curvatures, bifurcations and branches, subjected to low shear stress and disturbed blood flow (atherosclerosis prone areas)(Gimbrone et al 2000). In these atherosclerosis-susceptible sites, plasma cholesterol, mainly that circulating in LDLs, can accumulate in the sub-endothelial space of the arterial wall. When LDL particles become trapped in an artery, they can undergo modifications such as oxidation, enzymatic processing, desialylation and aggregation; the modified lipoproteins represent the primary source of lipid accumulation in atherosclerotic plaques (Krauss et al 2010). These alterations lead to the formation of pro-inflammatory particles inducing the expression of several cell surface adhesion molecules, chemokines and other mediators of inflammation. These conditions cause the migration of leucocytes from the circulation into the intima of the arterial wall. Once monocytes enter the intima, they differentiate into macrophages, under the influence of monocyte colony stimulating factor (M-CSF). Macrophages are the most abundant inflammatory cell type in plaques and have a central role in all stages of atherosclerosis development. At the beginning, the oxidation of LDL particles interfere with the interaction between LDLs and their receptors promoting the bind with scavenger receptors, SR-A and CD36, presented on the macrophage surface; with time these cells become laden with lipids. The uncontrolled up-take of ox-LDL, the excessive cholesterol esterification and the impaired cholesterol release, lead to the accumulation of CE; these are stored as lipid droplets resulting in the formation of foam cells, the major hallmarks of the early stage of atherosclerosis lesions (Ji et al 2011). Studies performed on mice lacking SR-A and CD36 receptors detected a modest decrease in atherosclerotic plaque (Suzuki H 1997). This early vascular lesion progresses further with the migration and proliferation of smooth muscle cells (SMC) from the media into the intima. These cells synthesize the bulk of the arterial extracellular matrix.

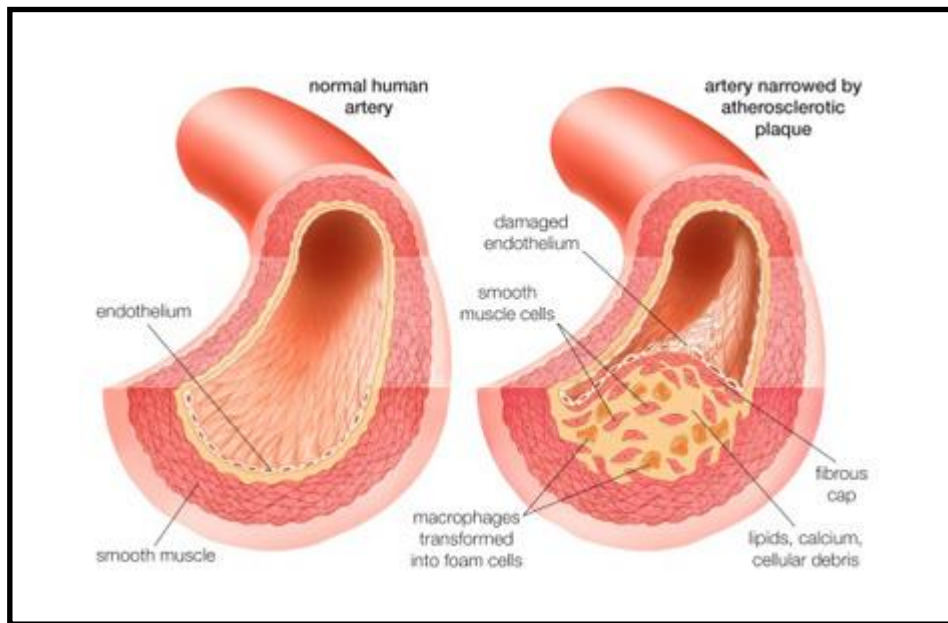


Figure 6. Representation of normal human artery and artery with atherosclerotic plaque.

Inflammation in Atherosclerosis

Inflammation is a process that plays a pivotal role in both the initiation and the progression of atherosclerosis (Rosenfeld et al 2013). Macrophages represent the main inflammatory cells, but other kinds of cells are involved in atherogenesis including dendritic cells (DCs), mast cells and T cells.

Intracellular cholesterol accumulated into macrophages can precipitate in the form of microcrystals able to activate an inflammasome, a cytosolic molecular machine that cleaves a proforma of interleukin (IL)-1 β , converting it into bioactive IL1 β that can be secreted by the cell (Duewell et al 2010). When released in the arterial intima, IL-1 β promotes the production of other pro-inflammatory molecules such as the cytokine IL-6 and the pro-inflammatory eicosanoid, PGE2 (Libby et al 1988). IL-1 β can also stimulate the expression of leucocyte adhesion molecules and matrix-degrading metalloproteinases. In this way cholesterol accumulation begets inflammation and tissue remodeling. Macrophages produces inflammatory cytokines that stimulate the generation of endothelial adhesion molecules, protease and other mediators, wich recruit T cells, B cells and other macrophages into the lesion site (Galkina et al 2009).

T lymphocytes are recruited in atherosclerotic lesions and are present at nearly all stages of their development. T cells are activated in atherosclerotic lesions by adhesion molecules and

chemokines. CD4⁺ T cells represent the most abundant T cells present in atherosclerotic lesions (Jonasson et al 1986). In the arterial vessel cholesterol accumulation and vascular inflammation lead to the differentiation of naïve CD4⁺T. T effector memory represent the subset of CD4⁺ T cells that support cytotoxic functions of CD8⁺T cells and produces cytokines such as IFN γ and IL4. They respond to local peptide antigens producing pro-inflammatory cytokines and contribute to atherosclerotic lesions formation and plaque vulnerability. These cells are routinely found in atherosclerotic plaques where they sustain the inflammatory response (Hansson et al 2006). On the other hand, regulatory T cells (Treg) inhibit this process displaying a protective effect on the development of atherosclerosis. T cells are responsible for the regulation of the pro-inflammatory phenotype of macrophages, through the production of interferon (IFN) and of cytokines such as TGF-beta and IL-10. CD8⁺T lymphocytes are less abundant than CD4⁺ cells, but are involved as well as in atherosclerosis development. They exert several effects during the atherosclerotic process including direct cytotoxicity and secretion of pro-inflammatory cytokines.

B lymphocytes are found in advanced atherosclerotic plaques, but their precise function is not known. These cells mediated adaptive immunity and can exert an atheroprotective role, in contrast to the pro-atherogenic role played by such inflammatory cells as monocytes and T-lymphocytes (Hansson 2002).

Plasmacytoid dendritic cells are a subset of dendritic cells that produces type I Interferon in response to virus; they present antigens on their surface and activate T cells (Reizis et al 2011) Dendritic cells have been observed in atherosclerotic lesions and in unstable plaques, suggesting that they are involved in atherosclerosis development in humans. Studies performed in atheroprone mice lacking plasmacytoid dendritic cells lead to the observation of a distinct decrease in lesion formation and a reduction of T cells infiltration in plaques (Döring et al 2012).

Mast cells contribute to innate and adaptive immunity and play an important function in inflammation while their products modulate the production inflammatory mediators. In health conditions mast cells are seldom observed in vascular sites. Their numbers within the arterial wall increases during atherosclerosis. Mast cells contribute to plaque destabilization by producing proteases such as tryptase and chymase which lead to intra-plaque hemorrhage, macrophages and endothelial cells apoptosis, matrix degradation, vascular leakage; they also produce cytokines

and chemokines, which bring about the recruitment of leukocytes to the atherosclerotic lesions (Zardi EM 2014).

Advanced Lesions in Atherosclerosis

Macrophage foam cells contribute to the further growth and destabilization of the plaque through the secretion of cytokines and chemokines, the production of reactive oxygen species (ROS), the presentation of immune activation markers to lymphocytes or to macrophage scavenger receptor, the generation of matrix-degrading proteases and the release of inflammatory debris into the atherosclerotic plaque core following necrosis or apoptosis (Randolph 2014). Cytokines and growth factors produced by macrophages and T cells stimulate migration and proliferation of vascular smooth muscle cells. The accumulation of these types of cells leads to the production of a complex of extracellular matrix composed of collagen, proteoglycans and elastin, eventually resulting in the formation of a fibrous cap (Libby 2000). When the macrophages lose the ability to accumulate more lipids, they degenerate and contribute to the formation of a necrotic core. Cell death can lead to necrosis by at least two mechanisms: apoptosis followed by defective phagocytic clearance ('efferocytosis') of the apoptotic cells and a process called primary necrosis (Libby et al 2014). The necrotic core is formed mainly by a lipid pool of esters of cholesterol and dead macrophages, which cause an additional recruitment of inflammatory cells (Seimon et al 2009).

The atherosclerotic process typically lies silent for months, years and even decades and may never result in clinical manifestations (Jonasson et al 1986). But once the surface of the plaque is damaged, thrombotic occlusion of the artery may ensue. Surface continuity can be damaged by fissuring (the so-called plaque rupture, observed in 60% to 80% of cases of acute coronary syndrome) or surface erosion (present in 20% to 40% of cases with coronary thrombosis (Farb et al 1996). Recent studies suggest that the proportion of infarctions caused by rupture versus erosion is changing, with more cases due to erosion and fewer to overt plaque rupture (Falk et al 2013). The sites of fatal disruption are characterized by a thin fibrous cap (<50–60 micrometers), depletion of SMC necessary to repair and maintain collagen, increase of inflammatory activity and heightened amounts of proteolytic enzymes (van der Wal et al 1994). Therefore, inflammatory stimuli such as local immune reactions might activate macrophages, mast cells and T cells to release cytokines that inhibit cap formation and proteases that digest fibrous components of the cap. Much interest has focused on the collagenolytic action of matrix metalloproteinases and

cysteine proteases in the plaque. (Sukhova et al 1998). Fissuring or erosion can lead to thrombus formation resulting in myocardial infarction and stroke (Virmani R 2002).

Murine models of atherosclerosis

Rodents, in particular mice, are the most useful experimental species for the study of several diseases, including atherosclerosis (Hofker MH 1998). The use of murine models presents both advantages and limitations (Table 2). Mice and humans show differences in parameters that influence atherogenesis and the distribution of the lesions. Humans present more atherosclerotic plaques in the coronary arteries, carotids and peripheral vessels such as the iliac artery. Conversely, mice manifest more frequently lesions in the aortic sinus, the site from which the ascending aorta originates. This area, due to its shape and position (next to the heart and exposed to high pressure with disturbed blood flow) proves to be subject to lipids accumulation. In mice, lesions can be present at other sites such as the arteries that pass from the aortic arch (brachiocephalic artery, left and right carotid arteries, right subclavia artery), the renal arteries and the aortic valves (Coleman et al 2006). The atherosclerotic lesions of mice do not exhibit such features associated with human disease as the unstable plaque with overlying thrombosis nor are characterized by the development of a thick fibrous cap.

Despite its limitations, the mouse represents the favorite species for the study of atherosclerosis, because it displays several advantages such as the ease of breeding, the ease of genetic manipulation and the ability to monitor atherogenesis within a reasonable time frame. In addition, mice and humans are genetically quite similar and share the same set of genes controlling lipoprotein metabolism. The reference mice, named wild-type, are characterized by a different lipoprotein profile compared to humans. In this model plasma cholesterol is essentially associated with the HDL fraction: therefore in the absence of atherogenic plasma lipoproteins, this mouse is resistant to atherosclerosis development. In addition, wild-type mice do not express CETP, which represent a potential target for atheroprotection in humans (Davidson et al 2010). About 30 years ago, it was observed that a variety of mice, named C57BL/6 for the colour of their fur, was able to develop moderate atherosclerotic lesions at the aortic sinus level, when fed with a diet high content in cholesterol. In more recent years, using the technique of homologous recombination, it was possible to generate murine models able to develop severe lesions along the arterial tree, both upon dietary challenge and spontaneously.

Advantages	Limitations
Ease of breeding/size of litters	No coronary lesions
Multiple inbred strains	Only partial resemblance to human
Short reproductive cycle	Limited tissue availability and technical difficulties due to small size
Relatively low cost of maintenance	Wild-type relatively atherosclerosis resistant
Well-known genome	Monotypic HDL
Ease of genetic manipulations to study the role of cell types or proteins on atherosclerosis	
Atherosclerosis develops over relatively short of time	
Useful for non-invasive imaging (MRI, PET; CT, Ultrasound)	

Table 2. Advantages and limitation of murine model of atherosclerosis

EKO mouse

In 1992 two different groups simultaneously generated the EKO mice by homologous recombination in embryonic stem cells. The EKO mouse, deficient in the apolipoprotein E, represents the most widely studied animal model for atherosclerosis (Zhang SH et al 1992)(Plump AS et al 1992). The deletion of the E gene leads to severe hypercholesterolemia with the development of spontaneous atherosclerotic lesions.

ApoE, a 34-kDa 299 amino acid long protein, is synthesized mainly in the liver but also in different cell types, including macrophages. This protein represents a constituent of plasma lipoproteins and plays an essential role in several anti-atherogenic functions through different mechanisms. ApoE is involved in the maintenance of cholesterol homeostasis, it serves as the ligand for the receptor-mediated up-take by the liver of circulating CMs, VLDL and their remnants, after their

binding to LRP and LDLR. This apolipoprotein exerts important functions in cholesterol metabolism and transport both stimulating reverse cholesterol transport and activating enzymes involved in lipoprotein metabolism such as hepatic lipase HL, CETP and LCAT. The process of cholesterol efflux is essential to maintain cholesterol homeostasis in cells that are incapable of limiting their uptake of lipids. Recent studies demonstrated that the secretion of apoE by macrophages stimulates cholesterol efflux via ABCA1. ApoE displays additional anti-atherogenic functions through various mechanisms including the inhibition LDL oxidation, the prevention of platelet aggregation and the reduction of the proliferation of T-lymphocytes, endothelial cells and SMCs (Greenow et al 2005).

EKO mice fed chow diet, a diet that contains low amount of fat and is almost free of cholesterol, display total cholesterol levels at least five-fold higher than their wild-type counterparts (300-500 mg/dl vs 100 mg/dl). In these animals cholesterol is mostly concentrated in CM and VLDL fractions and they develop spontaneous vascular atherosclerotic lesions. Over time, these lesions become more complex. When apoEKO mice are maintained with high-fat diet (a diet containing 0,2% cholesterol and 21% milk fat), they display a significant increase in plasma lipids with cholesterol about twenty times higher (> 1000 mg/dl) than the animals of the control group. Furthermore, the challenge diet induces accelerated and more severe atherosclerotic lesions. The lesions of animals fed high fat diet are richer in foam cells, while animals fed chow diet show complex cellular lesions (Imazuimi et al 2011). Foam cells lesions have been observed at 8 to 10 weeks of age in EKO fed chow diet. After 15 weeks intermediated plaque are present, containing spindle-shaped cells, in particular SMC. After 20 weeks, fibrous plaques are evident containing SMC, extracellular matrix and an overlying fibrous cap. This time course is accelerated by the high fat diet, with the more advanced lesions in these mice containing cholesterol crystals, a necrotic core and calcifications (Nakashima et al 1994).

A-IKO mouse

Apo A-I is constituted of 243 amino acid residues organized in amphipathic alpha helices, and is the main constituent of HDL, being essential for the biogenesis of these particles. ApoA-I plays a structural role in HDL and contributes as well as to their anti-atherosclerotic properties. It is synthesized and secreted by liver and intestine and is metabolized by the kidney. Hepatic apoA-I is synthesized as a preproprotein that is cleaved intracellularly by a signal peptidase. The resulting

propeptide is secreted before cleavage by bone morphogenic protein-1 in a process that is facilitated by procollagen C-proteinase enhancer (Chau et al 2007).

Epidemiological studies have demonstrated that HDL particles play a pivotal role against the development of atherosclerosis and cardiovascular disease, and high plasma levels of HDLs are inversely correlated with the incidence of these pathologies. This relationship can be explained, at least in part, with the atheroprotective effects of HDL lipoproteins. Its major protein component apoA-I mediates many HDL functions.

Over-expression of human apoA-I in C57Bl/6 mice, characterized by high plasma apoA-I and HDL levels, protects from atherosclerosis development (Rubin et al 1990). Another study, performed on transgenic mice over-expressing human apoA-I and with deletion of ApoE, showed a distinct decrease of atherosclerosis development, associated with a reduction in total cholesterol (577 mg/dl vs 663 mg/dl of EKO mice) and an increase in HDL-cholesterol (105 mg/dl vs 50 mg/dl) (Plump et al 1994)(Pászty et al 1994).

Mice lacking apoA-I (A-IKO) were generated in order to verify if a decrease of HDL lipoproteins can be involved in an increased predisposition to atherosclerosis development. These animals showed a marked reduction both in total plasma cholesterol and in HDL-cholesterol levels. In addition, the deficit of apoA-I led to increase in HDLs of apoA-IV and apoE, which under physiological conditions represent minor components of the particles. In apoA-IKO fed chow diet, the absence of apoA-I results in a reduction of total plasma cholesterol in comparison with the control group (23,7 mg/dL vs 90,2 mg/dL) and HDL-cholesterol (20 mg/dL vs 85,3 mg/dL). In mice between 8 and 15 months of age, fed chow diet, no atherosclerotic lesions were observed, while in animals fed the atherogenic diet for 32 weeks, only some pre-atherosclerotic lesions, such as foam cells at aortic valve level, were identified (Li H 1993). These studies demonstrated that in murine models, the decrease of apoA-I alone does not lead to atherosclerosis development in mice fed either chow diet or high fat diet.

LDLrKO/A-IKO mouse

LDLrKO represents another mouse model used to investigate atherosclerosis. When fed chow diet, this model develops atherosclerotic lesions only in older animals (Hartvigsen et al 2007). To obtain significant plaques the feeding of an atherogenic diet is necessary. Several studies have been

performed on the LDLrKO/apoA-IKO (dKO) murine model. After being maintained with atherogenic diet for 16 weeks, LDLrKO/A-IKO mice showed a lower increase of total plasma cholesterol (546 mg/dL female and 652 mg/dL male) in comparison with LDLrKO mice (2341 mg/dL female and 2226 mg/dL male). DKO animals develop markedly aortic atherosclerosis in response to an atherogenic diet. Furthermore, this model shows massive cholesterol accumulation in the skin, accompanied by an increase in dermal thickness, by hair loss and macrophage infiltration (Zabalawi M 2003).

Another study performed on the same model, showed, after 10 week on an atherogenic diet, an enlargement of skin draining lymph nodes in comparison with LDLR^{-/-} animals. In these lymphoid organs an accumulation of cholesterol and an expansion of the populations of T, B, dendritic cells and macrophages were observed (Wilhelm et al 2009).

The administration of lipid-free human apoA-I decreases inflammation and cholesterol accumulation in the skin and skin draining lymph nodes of LDLR^{-/-};apoA-I^{-/-} mice. In particular, the skin showed a reduction of cellularity and the restoration of skin architecture, morphology and composition. Furthermore, after the treatment a significant increase in the lymph nodes T reg population with a simultaneous reduction of T effectors were observed (Wilhelm et al 2010).

Murine models of coronary atherosclerosis

As mentioned previously, mouse models present limitations for the study of human cardiovascular disease. ApoEKO and LDLRKO, the traditional murine models of atherosclerosis, do not develop spontaneously coronary atherosclerotic plaques. However, in animals with additional genetic manipulation these lesions may be observed. ApoEKO/LDLRKO mice, maintained for 7 months with high fat diet, exhibit atherosclerotic plaque in coronary arteries and myocardial infarction, in particular when subjected to stress (Caligiuri et al 1999). Double knockout mice with homozygous null mutations for apoE and SR-BI genes, fed chow diet, display severe occlusive lesions in coronary artery at 5 weeks of age and develop multiple myocardial infarctions and cardiac dysfunctions including enlarged heart, reduced ejection fraction and contractility, and ECG abnormalities. All animals die by 8 weeks of age (Braun et al 2002). Also the SR-BIKO/LDLRKO animals, when fed a high fat diet, have accelerated atherosclerosis development at the aortic sinus and show coronary atherosclerosis (Fuller et al 2014).

AIM

Several studies have been showed that the concentration of HDL cholesterol (HDL-C) is inversely related to the risk of having a cardiovascular event. Moreover, increasing the levels of HDL lipoproteins and their main protein component apoA-I, which is directly involved in most of the anti-atherogenic properties of HDL, have been associated with a reduction in experimental atherosclerosis and a plethora of beneficial actions of HDL have been demonstrated in animal models. In this paradigm, HDL-C has been considered to be a marker of the potentially cardioprotective functions of HDL. However, recent studies have suggested that the mere concentration of HDL-C cannot always reflect HDL function, with growing evidence that under some conditions HDL functions can be compromised despite high concentration of HDL-C. Thus, a more complicated picture of the role of HDL apoA-I in cardiovascular disease prevention has emerged, also from recent studies performed in animal models where mice with target deletion of the murine apoA-I gene does not lead to a greater atherosclerosis susceptibility. For this reason there is a need for more critical evaluation of the different proposed functionalities of HDL, both in animals models and in the clinic. The aim of my project was to determine the effects of apoA-I on atherosclerosis development, phenotype, inflammation and immune function through the use of genetically modified mice deprived of, or overexpressing, apoA-I, in apoEKO background.

MATERIALS

&

METHODS

Mice

Procedures involving animals and their care were conducted in accordance with institutional guidelines that are in compliance with national (D.L. No. 26, March 4, 2014, G.U. No. 61 March 14, 2014) and international laws and policies (EEC Council Directive 2010/63, September 22, 2010: Guide for the Care and Use of Laboratory Animals, United States National Research Council, 2011). The experimental protocol was approved by the local authorities (Progetto di Ricerca Protocollo 2012/4).

C57Bl/6 (WT) and apoE knockout (EKO) mice were purchased from Charles River Laboratories (Calco, Italy). ApoE/apoA-I double knockout mice (EKO/A-IKO) and apoE/apoA-I double knockout mice overexpressing the human isoform of apoA-I (hA-I/EKO/A-IKO) were obtained by multiple crosses between EKO mice and apoA-I knock-out mice hemizygous for the expression of human apoA-I, previously generated in our lab.

Mouse apoE (For 5'-GCCTAGCCGAGGGAGAGCCG-3'; Rev1 5'-TGTGACTTGGGAGCTCTGCAGC-3'; Rev2 5'-GCCGCCCGACTGCATCT-3') and mouse apoA-I specific primers (For 5'-CCTTCTATCGCCTTCTTGACG-3'; Rev1 5'-GTTTCATCTTGCTGCCATACG-3'; Rev2 5'-TCTGGTCTTCTGACAGGTAGG-3') were used to screen by PCR the dKO and hA-I mouse lines.

Human apoA-I expression was assessed by Western blot analysis on mouse plasma, using a specific goat polyclonal antibody (cod. 600-101-109, Rockland Immunochemicals Inc. Limerick, PA, USA).

Mice were maintained under standard laboratory conditions (12 hours light cycle, temperature 22°C, humidity 55%), with free access to standard rodent chow (4RF21, Mucedola, Settimo Milanese, Italy) and tap water from weaning (8 weeks of age) to 30 weeks of age.

Harvesting of tissues

Mice were sacrificed at 30 weeks of age under general anaesthesia with 2% isoflurane (Forane, Abbot Laboratories Ltd, Illinois, USA). In advance of that, after an overnight fast, blood was collected, under 2% isoflurane anaesthesia, from the retro-orbital plexus into tubes containing 0.1% (w/v) EDTA and centrifuged in a microcentrifuge for 10 minutes at 5900 g at 4°C to obtain plasma samples.

Blood was removed from the body by perfusion with phosphate-buffered saline (PBS). For histological analyses, hearts were harvested, fixed in 10% formalin for 30 minutes and transferred into PBS containing 20% sucrose (w/v) overnight at 4°C before being embedded in OCT compound (Sakura Finetek Europe B.V., Alphen aan den Rijn, The Netherlands) and stored at -80°C.

From a first set of mice, one half of the spleen, as well as half of axillary and inguinal lymph nodes were harvested and immediately processed for flow-cytometry analysis. Contralateral skin draining lymph nodes (axillary and inguinal lymph nodes), and half the spleen were snap-frozen in liquid nitrogen for subsequent RNA-seq analysis.

From a second set of mice, axillary and inguinal lymph nodes, half of the spleen and liver were immersion-fixed in 10% formalin for 24 hours, dehydrated in a graded scale of ethanol, and paraffin embedded. Contralateral axillary and inguinal lymph nodes and half of the spleen were immersion-fixed in 10% formalin for 24 hours and transferred into PBS containing 20% sucrose (w/v) overnight at 4°C before being embedded in OCT compound and stored at -80°C.

Skin biopsies were harvested from two different anatomical areas (thoracic and abdominal regions), deep up to the muscle layer to be sure to include also hypodermis, and processed for both light and transmission electron microscopy for the evaluation of skin morphology at the structural and ultrastructural level.

Lipid/lipoprotein analyses

Total cholesterol was measured by an enzymatic method (ABX Diagnostics, Montpellier, France).

Plasma lipoprotein distribution was analyzed in plasma pools from three fasting mice for each mouse line. Plasma lipoproteins were separated by Fast Protein Liquid Chromatography (FPLC) with size exclusion method that separate lipoproteins according to their size. One Superose 6 10/300 (Pharmacia) column was utilized and 2 mM pH 7.4 Phosphate buffer containing 0.15 M NaCl, 0,03% EDTA and 0,02% NaN₃ was used as mobile phase. Plasma samples (500 µl) were introduced into the injector and carried into the column by the flowing solvent. Column was equilibrated with buffer before loading sample. Once in the column, the sample mixture separates as a

result of different components adhering to or diffusing into the gel. As the solvents is forced into the chromatographic bed by the flow rate, the sample separates into various zones of sample components and were detected by UV absorption at 280 nm. FPLC is performed at 0.5 mL/min constant flow rate for 120 minutes at room temperature. Forty fractions of 0.8 ml each were collected in 96 wells-plate and total cholesterol content was measured in each fraction as previously described.

Plasma hApoA-I concentration was determined by immunoturbidimetric assays, using an antiserum specific for human apoA-I (LTA, Italy). Coomassie staining was used to quantify plasma murine ApoA-I and to confirm the immunoturbidimetric quantification of hApoA-I.

Moreover, lipids were extracted from skin with a mixture of chloroform:methanol, lipid extracts were dried and the lipids dissolved using Triton X-100. Total and unesterified cholesterol, phospholipid and triglyceride contents were quantified by enzymatic assays and expressed as $\mu\text{g}/\text{mg}$ of tissue. Total cholesterol, unesterified cholesterol, triglycerides and phospholipids were quantified by enzymatic methods (ABX Diagnostics, Roche Molecular Biochemicals, ABX Diagnostics, B.L. Chimica, respectively). Esterified cholesterol content was calculated as total cholesterol – unesterified cholesterol.

En Face analysis

Aorta was rapidly dissected from the aortic root to the iliac bifurcation, periadventitial fat and connective tissue were removed as much as possible. Aorta was longitudinally opened, pinned flat on a black wax surface in ice cold PBS and photographed unstained for plaque quantification.

Aorta images were recorded with a stereomicroscope-dedicated camera (IC80 HD camera, MZ6 microscope, Leica Microsystems, Germany) and analyzed using ImageJ image processing program (<http://rsb.info.nih.gov/ij/>). An operator blinded to dietary treatment quantified the atherosclerotic plaques.

Histology

Heart. Serial cryosections (7 μm thick) spanning the entire length of the heart were cut. Every fifth slide was fixed and stained with hematoxylin and eosin (Bio-Optica,

Milano, Italy) to detect plaque area both at the aortic sinus and the coronary arteries level. Plaque area at the aortic sinus was calculated as the mean area of those sections showing the three cusps of the aortic valves. Adjacent slides were stained with Oil Red O to quantify intraplaque neutral lipid deposition (Sigma-Aldrich, St. Louis, MO, USA). The Aperio ScanScope GL Slide Scanner (Aperio Technologies, California, USA) was used to acquire digital images that were subsequently processed with the ImageScope software. A blinded operator to dietary treatment and genotype quantified plaque size.

Spleen, axillary and inguinal lymph nodes. Serial sections (4 μm thick) were obtained and stained with hematoxylin and eosin (Bio-Optica, Milano, Italy). A dedicated subset of spleen, axillary and inguinal lymph nodes was additionally included in OCT and cryosections (7 micron thick) were stained with Oil Red O to detect neutral lipid accumulation. Lipid deposition was measured as the percent of Oil Red O positive area over the total area. by the ImageScope software.

Skin. Skin samples (5 x 5mm²) were immersion-fixed in 4% paraformaldehyde buffered with PBS 0.1 M (pH 7.4) for 5hours at room temperature (RT), dehydrated in a graded scale of ethanol and paraffin embedded. Sections, 4 μm thick, were cut using a rotary microtome (RM2245, Leica Microsystems GmbH Wetzlar, Germany) and stained with hematoxylin and eosin. At least five non-consecutive slides for each sample were observed to evaluate the skin structure by a Nikon Eclipse E600 equipped with a Nikon digital camera DXM1200 (Nikon, Tokyo, Japan). The morphometric analysis of the skin of the four mouse lines was performed on hematoxylin and eosin-stained sections. Areas of epidermis, dermis, and hypodermis were separately measured on 10 slides per animal (from 3 mice of each genotype) using the software Image Pro-Plus (version 4.5.019; Media Cybernetics Inc., Silver Spring, MD, U.S.A.). Dermis/epidermis area ratio and hypodermis/epidermis area ratio excluding the dermal compartment were also calculated.

Transmission electron microscopy

Bioptic fragments (2 x 2mm²) were immersion-fixed overnight, at 4°C, in 3% glutaraldehyde diluted in 0.1 M Sorensen phosphate buffer (pH 7.4), washed three times for 30 min each with Sorensen phosphate buffer, and post-fixed in 1% Osmium

Tetroxide. After dehydration through an ascending series of ethanol solutions, samples were embedded in Durcupan (Durcupan, Fluka, Milan, Italy). Semithin sections, 2 μm thick, were stained with toluidine blue. Ultrathin sections were obtained with an Ultracut ultramicrotome (Reichert Ultracut R-Ultramicrotome, Leika, Wien, Austria) and stained with uranyl acetate/lead citrate before observation by a Jeol CX100 transmission electron microscope (Jeol, Tokyo, Japan).

Flow-cytometry analysis

Several leukocytes populations were investigated by flow cytometry. CD4⁺ T lymphocyte subsets, T naïve (TNAIVE); T Central Memory (TCM), T Effector Memory (TEM), were analysed by flow cytometry in peripheral blood, spleen and lymph nodes. In addition, the attention were also focused on monocytes, monocytoïd as well as plasmacytoïd dendritic cells and B cells both in blood and secondary lymphoid organs. For flow-cytometry analysis a Calibur Flow Cytometer (BD Biosciences) with two lasers was used. The panels consisted of the subsequent cellular surface markers: CD4 (PE YTS 191.1.2, Immunotools), CD44 (FITC, IM7, BD Pharmigen), CD62L (APC, mMEL-14, BD Pharmigen), Ly-6C (FITC AL-21, BD Pharmigen), CD115 (APC AF598, eBioscience), CD11b (PE M1/70.15, Immunotools), CD11c (APC HL3, BD Pharmigen), B220 (PerCP Cy5,5 RA3-6B2, BD Pharmigen), CD19 (FITC 1D3, BD Pharmigen) and CD5 (APC 53-7.3, BD Pharmigen). All data were acquired in FCS format and were processed and analyzed using FCS Express V3 Research edition (De Novo Software, Inc; www.denovosoftware.com). CD4⁺CD44⁻CD62L⁺ are indicated as T naïve, CD4⁺CD44⁺CD62L⁻ are indicated as T effector memory cells and CD4⁺CD44⁺CD62L⁺ are indicated as T central memory cells. CD11b⁺CD115⁺Ly6C^{lo} are indicated as patrolling monocytes and CD11b⁺CD115⁺Ly6C^{hi} as inflammatory monocytes. CD11c^{hi}CD11b⁺B220^{lo} are indicated as myeloid while CD11c^{lo}CD11b⁺B220^{hi} as plasmacytoïd dendritic cells. CD19⁺CD5⁺ are indicated as B1a cells and CD19⁺CD5⁻ as B1b cells.

RNA extraction from lymphoid organs

Total RNA was isolated from axillary/inguinal lymph nodes and spleen of EKO/A-IKO and hA-I/EKO/A-IKO mice using the NucleoSpin RNA extraction kit (Macherey-Nagel,

Duren, Germany) according to the manufacturer's instructions. RNA concentration and purity were estimated evaluating the ratio of optical density at 260 and 280 nm (Nanodrop 1000, ThermoScientific, Wilginton, DE). RNA integrity was checked by electrophoresis in a 1.7% TAE gel stained with ethidium bromide (Sigma-Aldrich, Seelze, Germany).

RNA-seq analysis

For RNA-Seq analyses, the quality of the mRNA was also tested using the Agilent 2100 Bioanalyzer (Agilent Technologies, Santa Clara, CA). RNA samples were processed using the RNA-Seq Sample Prep kit from Illumina (Illumina, Inc., CA, USA). 8 to 9 tagged libraries were loaded on one lane of an Illumina flowcell, and clusters were created using the Illumina Cluster Station (Illumina, Inc., CA, USA). Clusters were sequenced on a Genome Analyzer IIx (Illumina, Inc., CA, USA) to produce 50nt single-end reads.

Bioinformatics analysis

Pre-processing of reads. A custom script implementing strict quality filters based on the provided base call quality scores was used to trim sequence reads prior to assembly. Reads were iteratively trimmed from the 3' end until all of the following conditions were satisfied:

1. the median quality score (Qscore) of upstream bases was >25
2. less than 3 bases with Qscore ≤ 10 and less than 5 bases with Qscore ≤ 20 were present in the upstream sequence
3. the cumulative error probability in the upstream region was below $5E-3$.

Only reads longer than 40nt in length after trimming were retained.

Differential gene expression. Reads were mapped to the mouse genome (mm10) using the TopHat2 software (23618408) in conjunction with the reference Refseq annotation (excluding tRNA and rRNA genes). Differentially expressed genes were identified using CuffDiff (23222703).

Functional association analysis

Lists of differentially expressed genes were uploaded into the Database for Annotation, Visualization and Integrated Discovery (DAVID) v6.8 Beta ([https://david-ncifcrf.gov/](https://david.ncifcrf.gov/)) (Nature Protocols 2009; 4(1):44 & Nucleic Acids Res. 2009;37(1):1) to determine differentially regulated pathways using the mouse genome as reference background. Data were analyzed with the Functional Annotation Chart tool using the KEGG pathway or the Biological Process Gene Ontology term. Cutoff criteria used were either a Benjamini multiple testing correction p-value less than 0.05 or a modified Fisher's exact (EASE score) p-value of less than 0.01.

Statistical analyses

Data are expressed as mean \pm SD. Group differences were tested for statistical significance by ANOVA, followed by Tukey post hoc test. A value of $p < 0.05$ was considered statistically significant. statistical analyses were performed using the SYSTAT software (Version 13; Systat Software, Inc., Chicago, IL).

RESULTS

Plasma cholesterol profile and apoA-I concentration

Plasma cholesterol concentration in EKO/A-IKO mice was significantly increased compared with that of WT mice (109.24 ± 10.18 mg/dl vs. 83.91 ± 5.97 mg/dl, respectively; $p < 0.01$), and approximately 4-fold lower than the concentration observed in EKO mice (109.24 ± 10.18 mg/dl vs. 397.94 ± 31.09 mg/dl; $p < 0.01$) and hA-I/EKO/A-IKO mice (109.24 ± 10.18 mg/dl vs. 441.31 ± 137.37 mg/dl; $p < 0.01$).

To evaluate the cholesterol distribution among the different lipoprotein classes, mouse lipoproteins were separated by FPLC and the cholesterol content was measured on the collected fractions. The cholesterol profile of WT mice was characterized by a cholesterol distribution almost exclusively confined to the HDL fraction, whereas EKO mice displayed a major cholesterol accumulation in the VLDL/LDL fractions and lower HDL-cholesterol levels compared WT mice. In EKO/A-IKO mice, HDL-cholesterol was almost absent and the cholesterol accumulation in the VLDL/LDL fractions was lower than that found in EKO mice. hA-I/EKO/A-IKO mice were on the contrary characterized by a large HDL-cholesterol peak and by a marked presence of VLDL/LDL particles, although less prominent than in EKO mice (Figure 7).

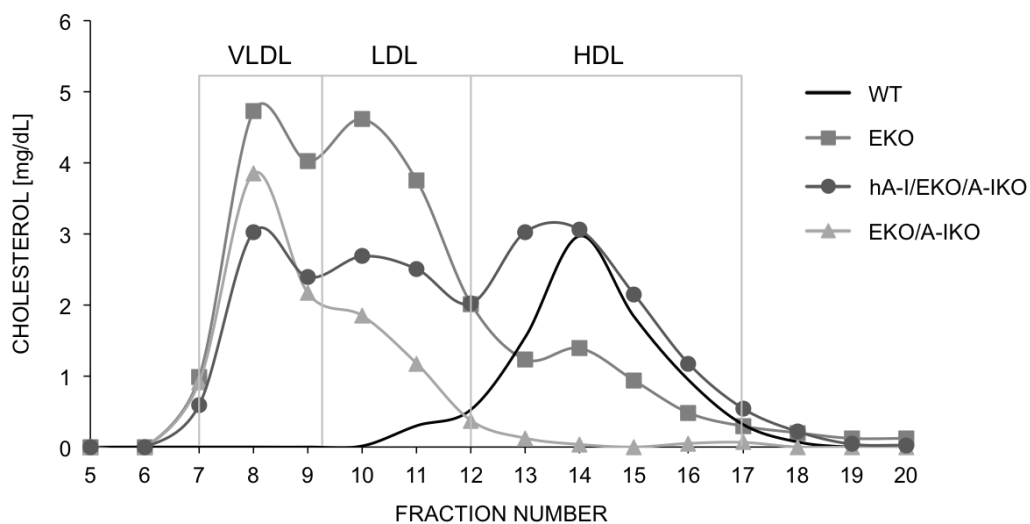


Figure 7. Cholesterol FPLC profile in mice plasma. Plasma lipoprotein were separated by size exclusion chromatography and the cholesterol content was measured in each fraction.

ApoA-I concentration in EKO mice was approximately 2.6-fold reduced compared with that measured in WT mice (39.3 ± 4.5 mg/dl vs 103.2 ± 12.7 mg/dl, respectively). In contrast, hA-I/EKO/A-IKO mice showed a concentration of apoA-I 5.4-fold higher than that found in EKO mice and 2-fold higher than that found in WT mice (212.1 ± 75.5 mg/dl). As expected, plasma apoA-I was completely depleted in EKO/A-IKO mice.

Atherosclerosis evaluation

To investigate the role played by different levels of apoA-I during atherosclerosis development, EKO/A-IKO, hA-I/EKO/A-IKO, EKO and WT mice were fed chow diet for 22 weeks. Atherosclerotic burden was quantified at the aortic sinus by histology and in the whole aorta by en-face analyses.

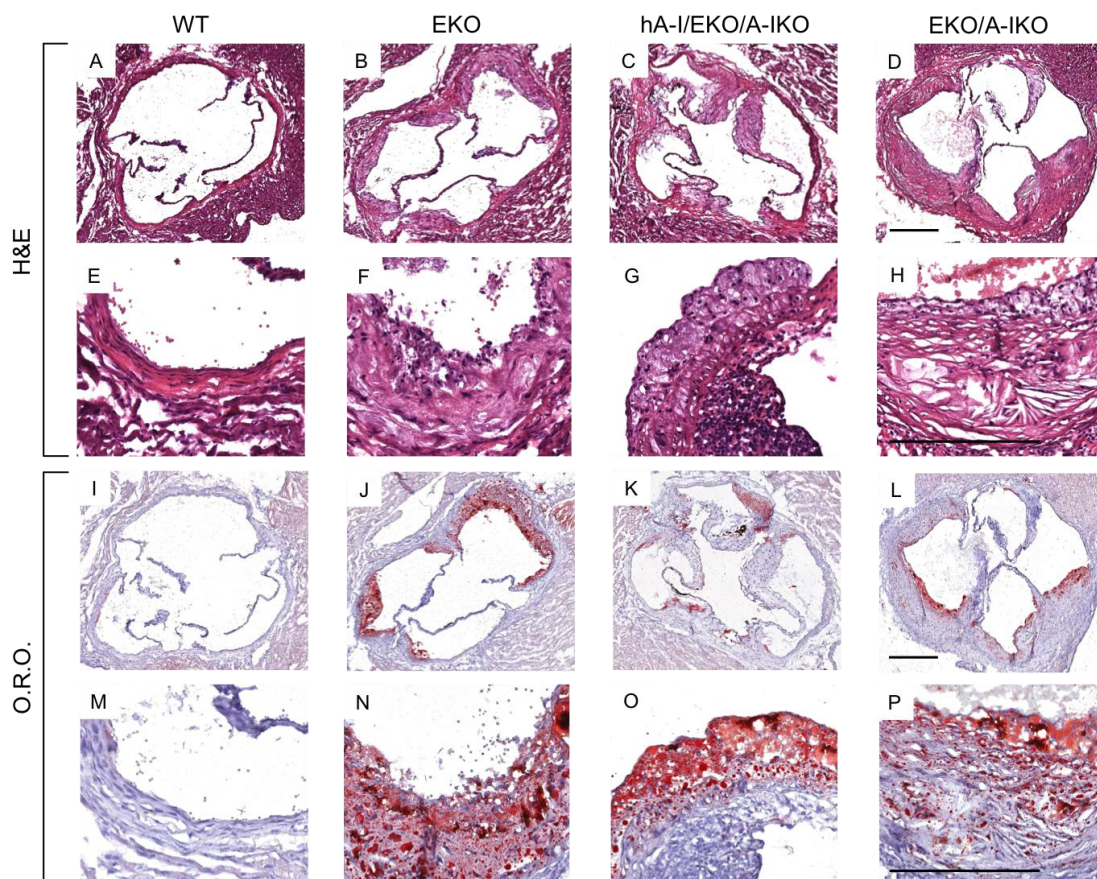


Figure 8. Histological characterization of plaques in the aortic sinus stained both with hematoxylin&eosin (A-H) and Oil Red O (I-P) in all experimental group fed with chow diet for 22 weeks (Bar = 250 μ m)

Aortic sinus histology. The deficiency of apoA-I caused a worsening in plaque development at the aortic sinus of in EKO/A-IKO mice compared with EKO mice ($3.2 \pm 0.7 \times 10^5 \mu\text{m}^2$ vs. $6.2 \pm 0.5 \times 10^5 \mu\text{m}^2$, respectively; $p < 0.001$). Conversely, hA-I overexpression dramatically reduced atherosclerotic plaque development at the aortic sinus of hA-I/EKO/A-IKO mice compared with both EKO/A-IKO ($0.5 \pm 0.3 \times 10^5 \mu\text{m}^2$ vs. $6.2 \pm 0.5 \times 10^5 \mu\text{m}^2$, respectively; $p < 0.001$) and EKO mice ($0.5 \pm 0.3 \times 10^5 \mu\text{m}^2$ vs. $3.2 \pm 0.7 \times 10^5 \mu\text{m}^2$, respectively; $p < 0.001$). As expected, no plaques were observed at the aortic sinus of WT mice (Figure 8).

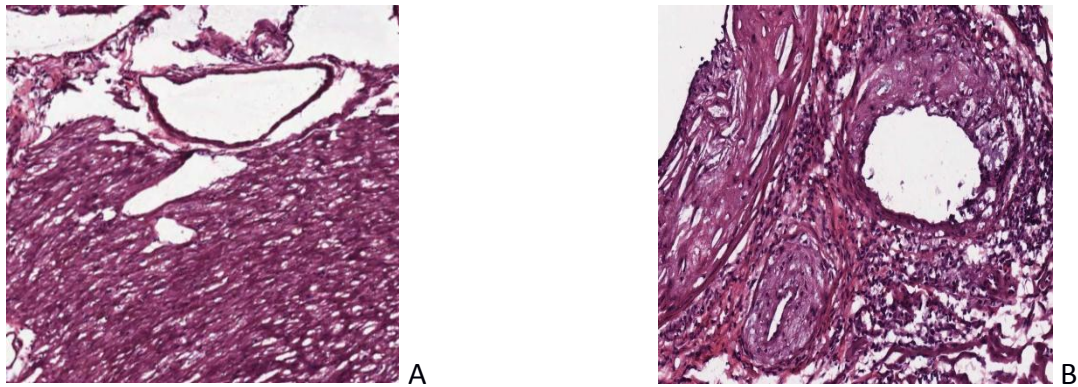


Figure 9. Histological characterization of plaques in the common coronary arteries stained with hematoxylin&eosin in EKO mice (A) and EKO/A-IKO mice (B).

Coronary arteries histology. In addition, preliminary data suggest that EKO/A-IKO, but not apoEKO develop significant atherosclerotic plaques at the common coronary arteries ($76,25 \pm 8,62\%$ and $0 \pm 0\%$, respectively) (Figure 9 A-B).

En Face analysis. En face analysis demonstrated that apoEKO/apoA-IKO and apoEKO mice had a similar extent of atherosclerotic plaques at the aortic arch ($6.9\pm 5.6\%$, $7.2\pm 5.5\%$, respectively; $p>0.05$) whereas no plaque development was observed at the aortic arch of hA-I/EKO/A-IKO and WT mice. No atherosclerosis was observed in thoracic and abdominal aortic segments, regardless of genotype (Figure 10).

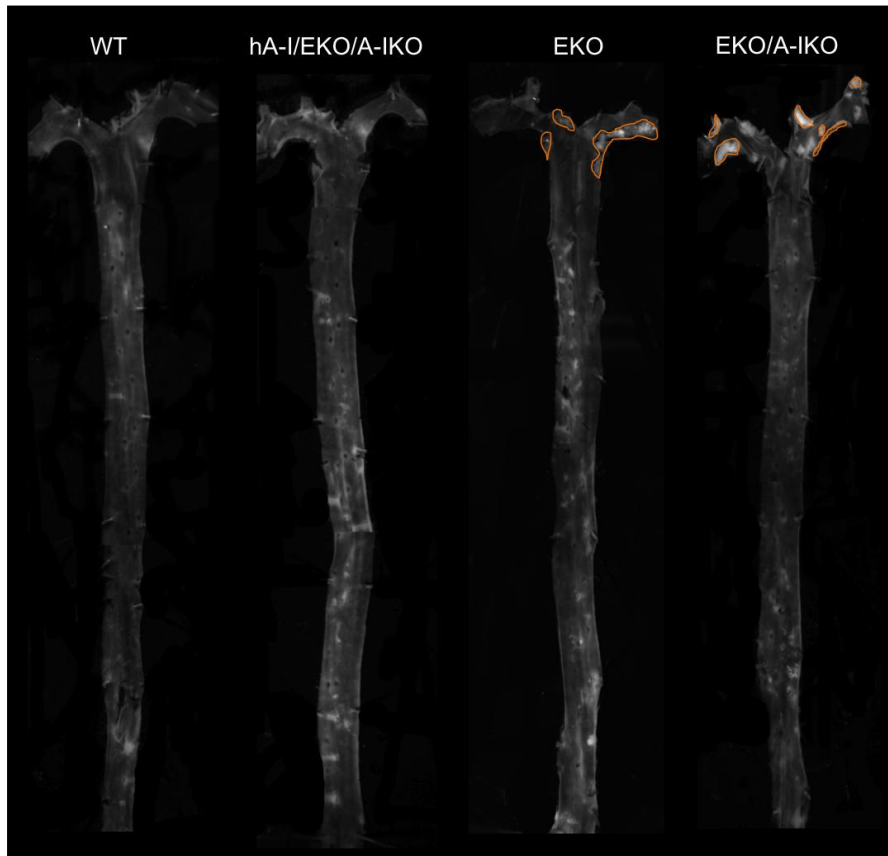


Figure 10. En face analysis of the whole aorta in all experimental groups.

Skin phenotype

The skin of EKO/A-IKO animals showed macroscopic alterations that were not present in all the other experimental groups (Figure 11). Particularly, in these mice, hair loss and a pale/yellowish color of the skin was observed, mainly at the ventral region. No ulcerated skin lesions and excoriations were present (Figure 11).



Figure 11. Macroscopic representation of the cutaneous phenotype.

Light microscopy analysis confirmed a great reduction of hair follicles in EKO/A-IKO mice if compared with WT, EKO and hA-I/EKO/A-IKO mice (Figure 12 A-B). On the other hand, epidermis showed comparable features and structure in all the considered groups. Dermis of EKO and hA-I/EKO/A-IKO mice was not different from that of WT mice (Figure 12 C D). In EKO/A-IKO mice, the dermis was thickened. Semithin sections revealed the presence of cholesterol clefts in papillary dermis (Figure 12 E) and foam cells accumulation in reticular dermis (Figure 12 F).

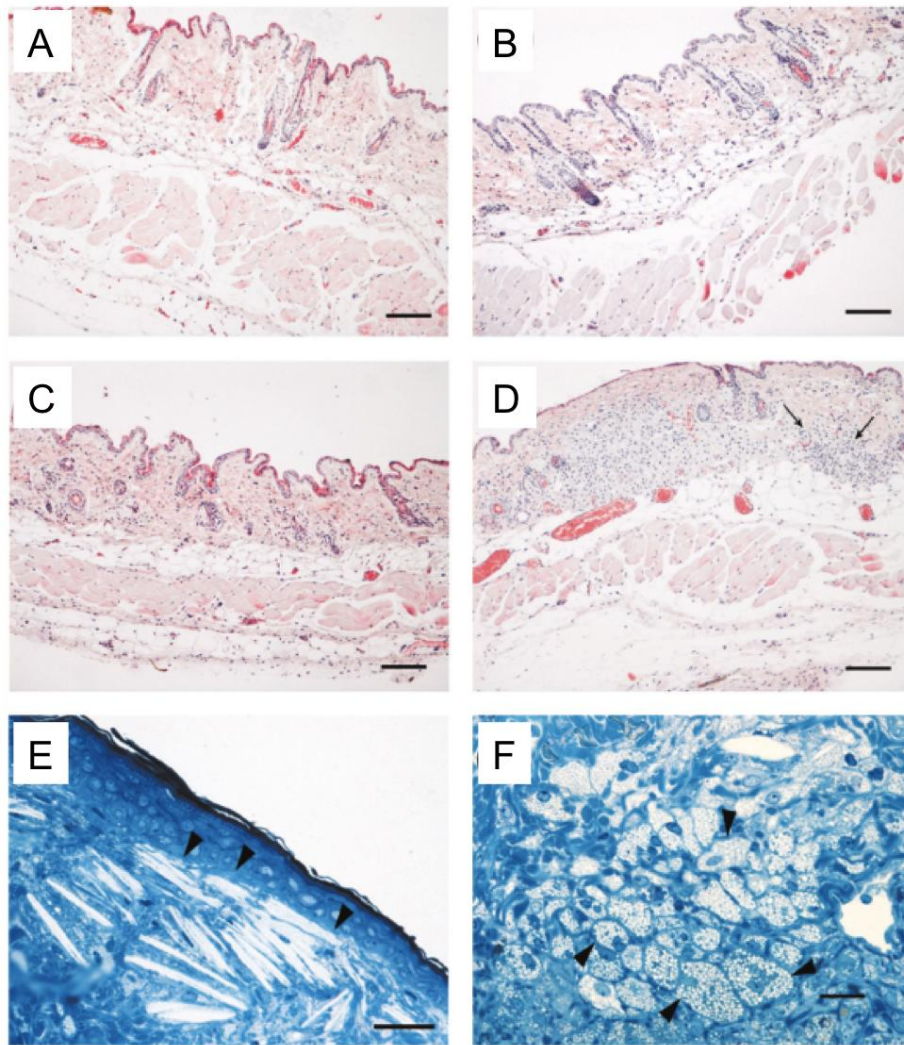


Figure 12. Skin histology. Light microscopy analysis. Representative photomicrographs of mouse skin. (A–D): paraffin sections after haematoxylin and eosin staining; (E and F): araldite semithin sections after toluidine blue staining. (A): WT mice; (B): EKO mice; (C): hA-I/EKO/A-IKO mice; (D–F): EKO/A-IKO mice. In (D) arrows indicate leukocyte infiltration; arrowheads indicate in (E) cholesterol clefts and in (F) foam cells. Bars: (A–D): 60 μm ; (E): 15 μm ; (F): 10 μm .

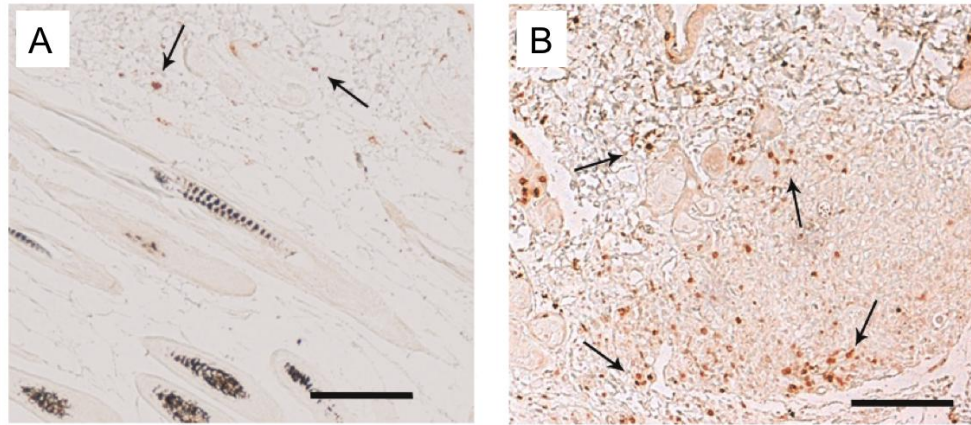
Quantification of the skin lipid content of WT and EKO/A-IKO mice showed a strong accumulation of both unesterified and esterified cholesterol in EKO/A-IKO mouse skin (Table 3).

	WT	EKO/A-IKO
Total cholesterol	1.53±0.43	7.69±1.90*
Unesterified cholesterol	1.43±0.41	5.96±1.42*
Esterified cholesterol	0.10±0.08	1.73±0.53*
Phospholipids	3.85±0.97	6.24±2.15
Triglycerides	14.98±7.69	22.31±13.44

Table 3. Skin lipid content of C57/Bl6 and A-IKO/EKO mice.

*Data are expressed as μg of lipid/mg of tissue. Results are shown as mean \pm SD (n=5), *p<0.01 vs C57BL/6*

Immunohistochemical analysis revealed just some scattered CD3-positive cells localized in the papillary dermis in the skin of WT mice (Figure 13 A), while, in EKO/A-IKO mice, CD3-positive cells were present in the papillary dermis and were organized in clusters in the reticular dermis, especially close to foam cells (Figure 13 B). In WT mice the expression of F4/80 was absent (Figure 14 A). On the other hand this immunostaining in EKO/A-IKO mice was well visible, particularly in the reticular dermis where foam cells accumulated, suggesting their macrophagic origin (Figure 14 B).



C

	C57Bl/6	A-IKO/EKO
Papillary dermis	+	++
Reticular dermis	0	+++

0: negative staining; +: weakly positive; ++: moderate positive; +++: strongly positive.

Figure 13. Skin IHC CD3. CD3 immunohistochemical and semi-quantitative analysis. (A and B). Representative photomicrographs of mouse skin paraffin sections after anti-CD3 immunostaining. (A): C57BL/6 mice; (B): EKO/A-IKO mice. Arrows indicate CD3 positive cells. (C):Semi-quantitative evaluation of CD3 staining. Bars: 60 μ m.

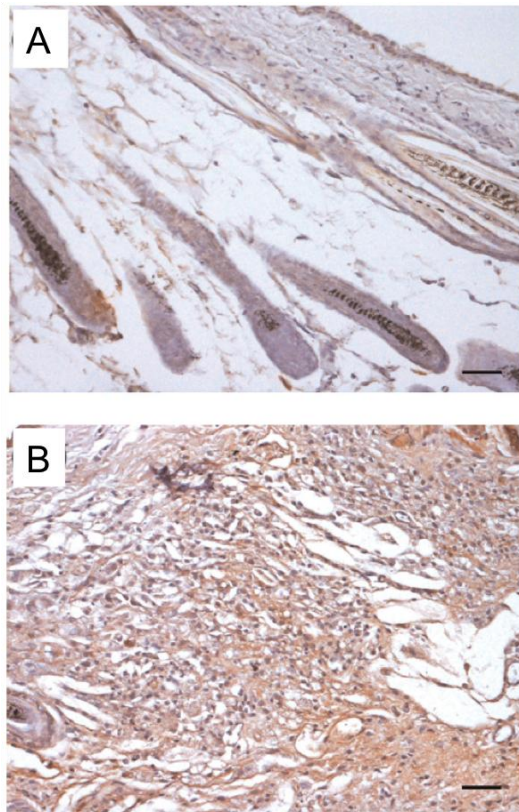


Figure 14. F4/80 immunohistochemical analysis. Representative photomicrographs of mouse skin paraffin sections after anti-F4/80 immunostaining. (A): WT mice; (B): EKO/A-IKO mice. Bars:30 μ m.

Morphometric analysis demonstrated that both epidermis and hypodermis areas were comparable in all the considered groups. Hypodermis thickness was comparable in all groups, and the hypodermis/epidermis area ratio in EKO/A-IKO and WT mice were not different (3.02 ± 0.14 vs. 3.44 ± 0.21 , respectively; $p > 0.05$).

Accordingly with light microscopy observations on haematoxylin/eosin and semithin sections, showing a thickened dermis in EKO/A-IKO mice, the dermis/epidermis area ration in this mouse line was much higher compared to all the other mouse lines (36.21 ± 3.71 in EKO/A-IKO; 16.45 ± 6.25 in WT; 15.59 ± 1.42 in EKO; 16.84 ± 0.43 in hA-I/EKO/A-IKO; $p < 0.0001$).

TEM analysis confirmed that the epidermis was well preserved and comparable among the different experimental groups (Figure 15). Epidermal layer count revealed, in all the four different group, three keratinocyte layers. The basal membrane was always continuous and no detachments between the epidermis and

the underlying dermis occurred. In EKO/A-IKO animals, immediately below the keratinocyte basal layer, large cholesterol clefts were present and arranged parallel to the epidermal surface (Figure 15).

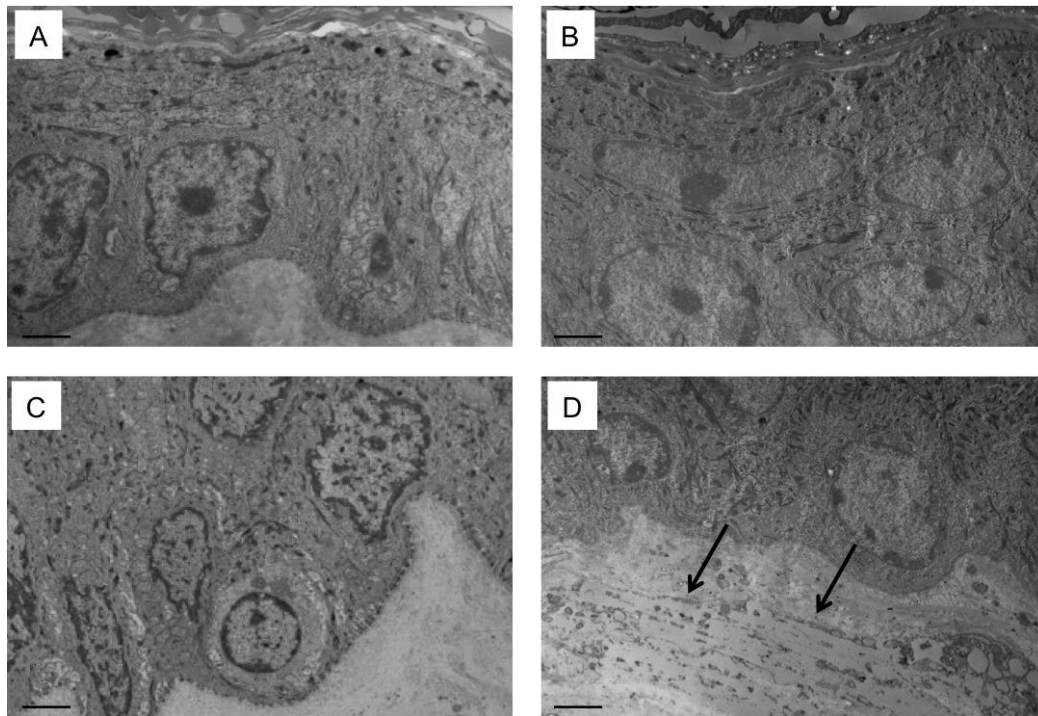


Figure 15. Transmission electron microscopy analysis of epidermis and papillary dermis. Representative photomicrographs of murine skin araldite ultrathin sections. (A): WT mice; (B): EKO mice; (C): hA-I/EKO/A-IKO mice; (D): EKO/A-IKO mice. In (D) arrows indicate cholesterol clefts. Bars: 2 μ m.

Interestingly, in the reticular dermis, where foam cells accumulated (Figure 16 A-B), intracellular cholesterol clefts were found inside these cells (Figure 16 C). Herein, these sharp and elongated structures were very much smaller than those located in the extracellular matrix of the papillary dermis when observed at the same magnification.

Foam cells did not show any contractile fibrils inside their cytoplasm, thus suggesting their macrophagic origin (Figure 16). Moreover, consistent with CD3 immunostaining, T lymphocytes were identified in the reticular dermis where foam cells accumulated (Figure 16 D), supporting the occurrence of a possible inflammatory response.

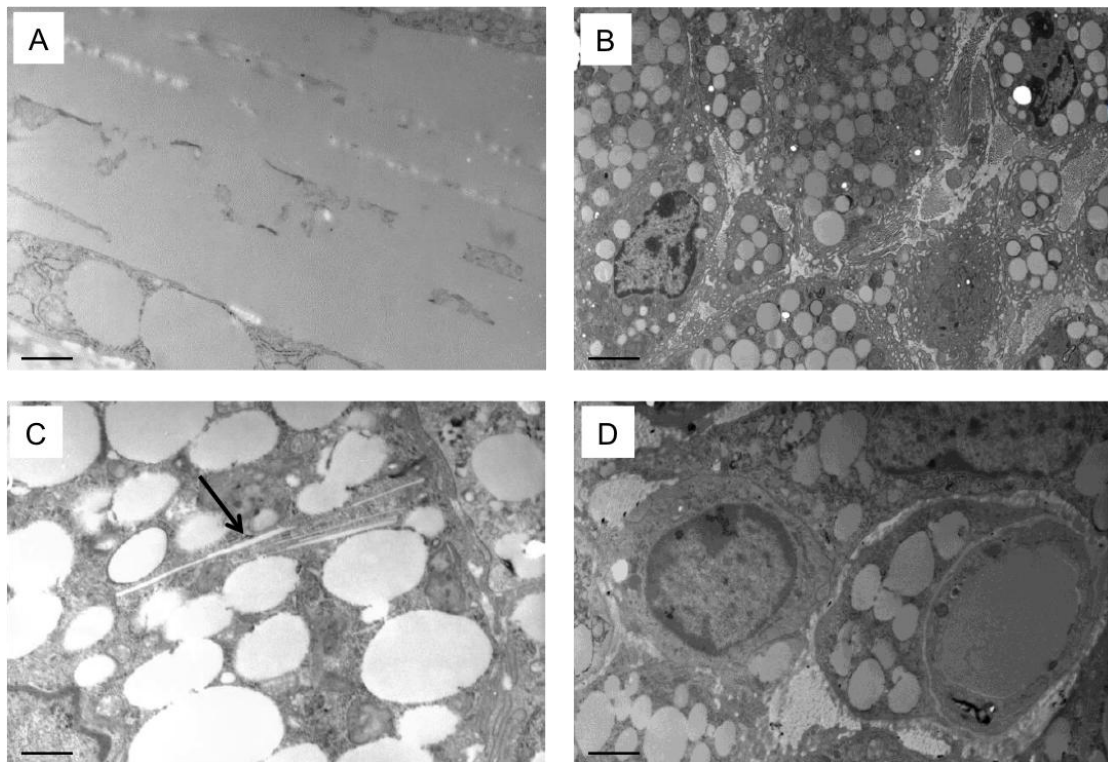


Figure 16. Transmission electron microscopy analysis of reticular dermis in EKO/A-IKO mice. Representative photomicrographs of skin araldite ultrathin sections. (A): extracellular cholesterol clefts; (B): foam cells; (C): intracellular cholesterol clefts; (D): a foam cell and a lymphocyte. In (C) arrow indicates cholesterol clefts. Bars: (A and C): 500nm; (B): 2 μ m; (D):1 μ m.

Secondary lymphoid organs phenotype and histology

Among the athero-protective effects displayed by apoA-I/HDL, a growing importance is attributed to its immunomodulatory role. To this aim, a macroscopic and histological characterization of different lymph nodes and spleen has been performed in all the mouse lines.

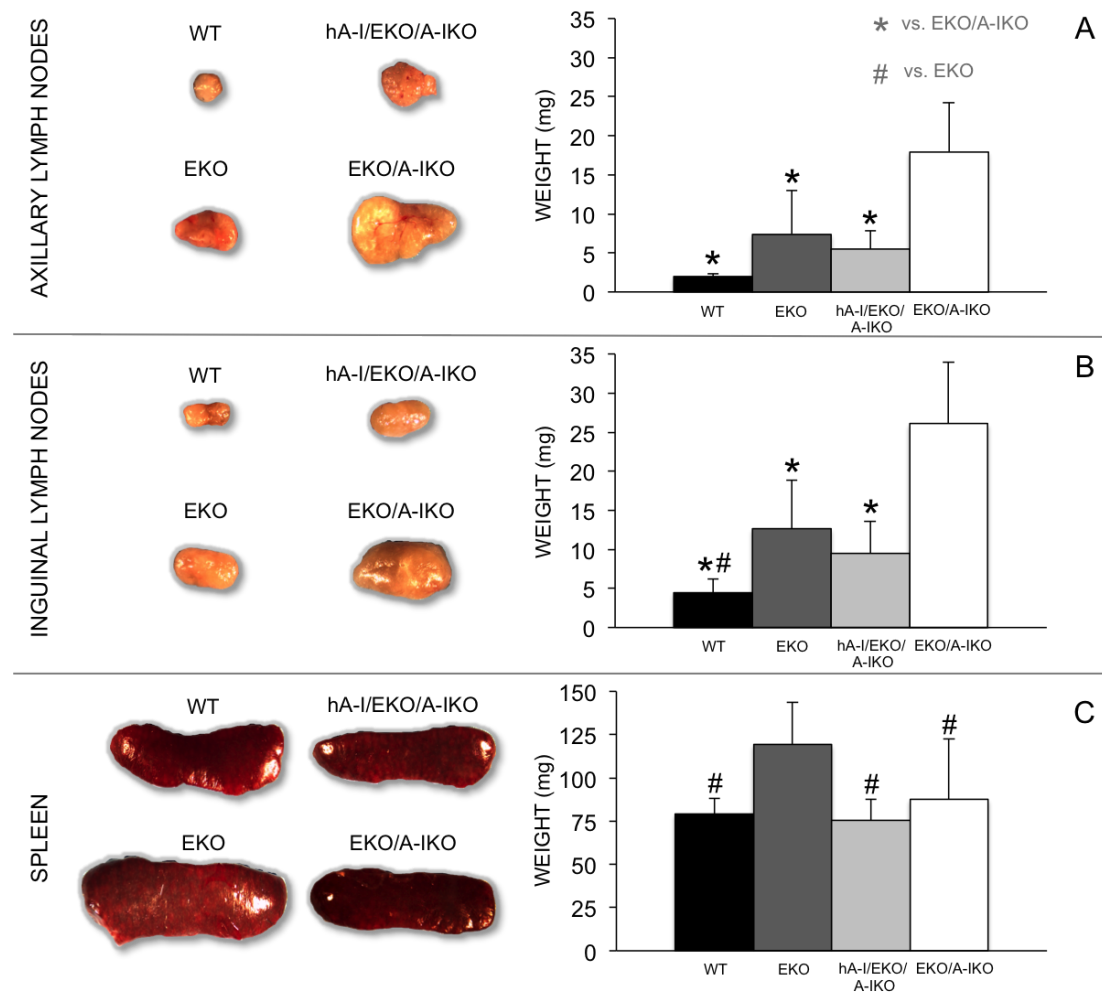


Figure 17. Figure 19. Weight of axillary and inguinal lymph nodes and spleens in all experimental groups after 22 weeks on regular chow diet.

EKO/A-IKO mice were characterized by a significantly higher weight of both axillary and inguinal lymph nodes compared with the other mouse lines (Fig. Panel lymphoid organs). On the contrary, the weight of the spleen from EKO/A-IKO mice was comparable with those from hA-I/EKO/A-IKO mice and WT mice, whereas a significant increase in spleen weight was observed in EKO mice (Figure 17. Panel lymphoid organs).

Histological analyses revealed that EKO/A-IKO mice had a dramatic increase in the amount of macrophages and granulocytes within the lymph node parenchyma in comparison with all the other genotypes (Fig. EKO/A-IKO detail). Moreover, three main features were observed specifically in EKO/A-IKO mice: i) large macrophages, often characterized by a foamy cytoplasm, were seen as single cell or in small group

in the cortex, surrounded by lymphoid cells (Fig. EKO/A-IKO detail) presence of granulomatous reactions in the inner cortex and the medulla, localized around a large number of multinucleated macrophages and cholesterol crystals (Fig. EKO/A-IKO detail); iii) dilation of subcapsular, cortico-medullary and medullary sinuses (Figure 18).

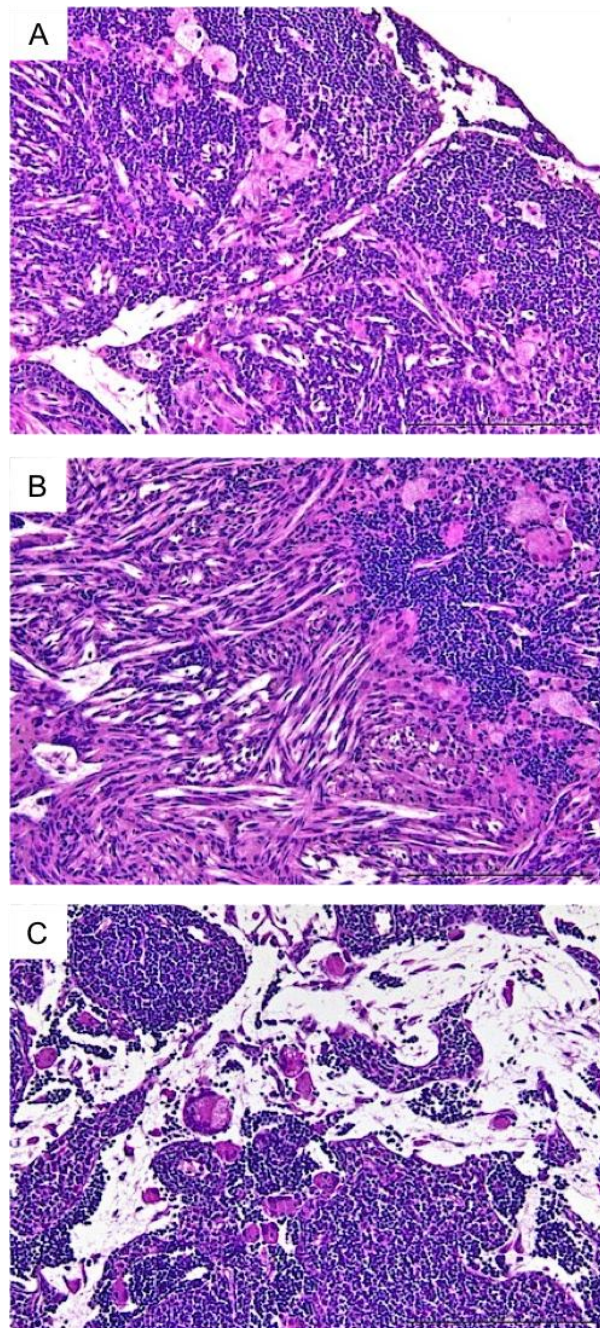


Figure 18. Histological representation of lymph nodes of EKO/A-IKO mouse stained with hematoxylin & eosin. Large foamy macrophages (A); granulomatous reaction centered around elongated empty spaces reminiscent of cholesterol crystals (B);

dilatation of sinuses presence of multinucleated foamy macrophages within the lumen of sinuses (C).

In addition, neutral lipid-specific staining with Oil-Red-O indicated that WT mice had the lowest lipid deposition, measured as % of surface positive to O.R.O. staining (axillary lymph node: 0.8 ± 0.33 %; inguinal lymph node: 1.28 ± 0.3 %); EKO and hA-I/EKO/A-IKO had a comparable lipid deposition (axillary lymph node: 1.35 ± 0.63 % and 2.28 ± 0.88 %, respectively; inguinal lymph node: 1.63 ± 0.58 % and 3.22 ± 1.67 %, respectively); whereas EKO/A-IKO mice had significantly increased lipid deposits compared with all the other genotypes (axillary lymph node: 12.17 ± 5.53 %; inguinal lymph node: 14.29 ± 7.69 %) (Figure 19).

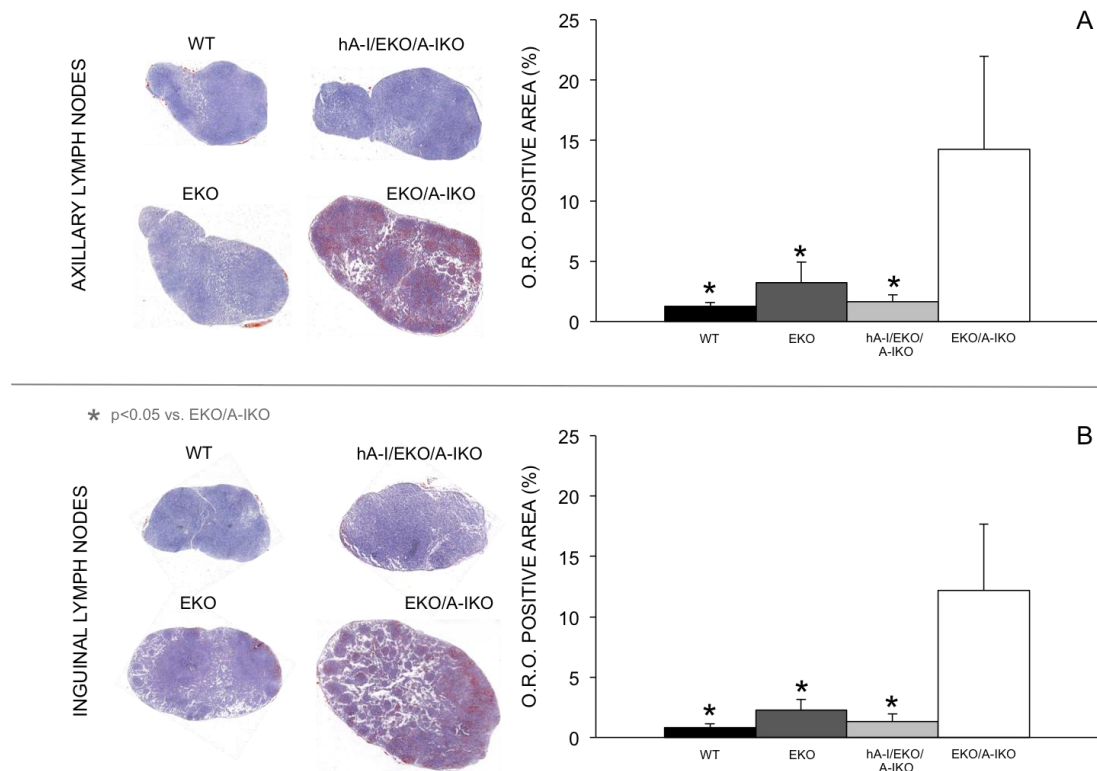


Figure 19. Histological representation of lymph nodes of all experimental group stained by Oil Red O.

Both spleen histology and splenic lipid deposition resulted unaffected by genotype (Figure 20).

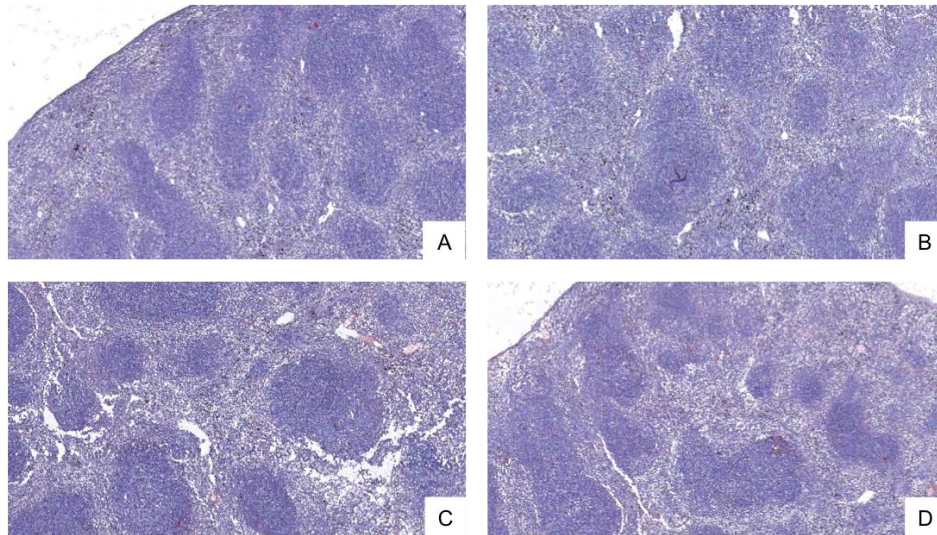


Figure 20. Histological representation of spleen of all genotypes. (A): WT mice; (B): EKO mice; (C): hA-I/EKO/A-IKO mice; (D): EKO/A-IKO mice.

Leukocytes subsets

The analysis of CD4⁺ T cell subsets (T naïve, T central memory cells, T effector memory cells) revealed that, in peripheral blood and spleen, EKO/A-IKO mice had a significantly increased percentage of T effector memory cells and a significantly reduced percentage of T naïve compared with the other genotypes (Figure 21). Concomitantly, WT mice had the highest percentage of T naïve compared with all the other genotypes (Figure 21). In the axillary lymph node, EKO/A-IKO mice had a significantly increased percentage of T effector memory cells compared with the other genotypes and a significantly reduced percentage of T naïve, compared with WT mice (Figure 21). Interestingly, in the inguinal lymph node of EKO/A-IKO mice, only a tendency toward an increased percentage T effector memory cells was detected (Figure 21). The percentage of T central memory cells resulted always unaffected by genotype (Figure 21).

Moreover, the relative abundance of monocyte subsets (inflammatory vs. patrolling) in peripheral blood (Figure 22), as well as the percentage of monocytoid/plasmacytoid dendritic cells (Figure 23) and B1a/B1b lymphocytes in secondary lymphoid organs was unaffected by genotype (Figure 24).

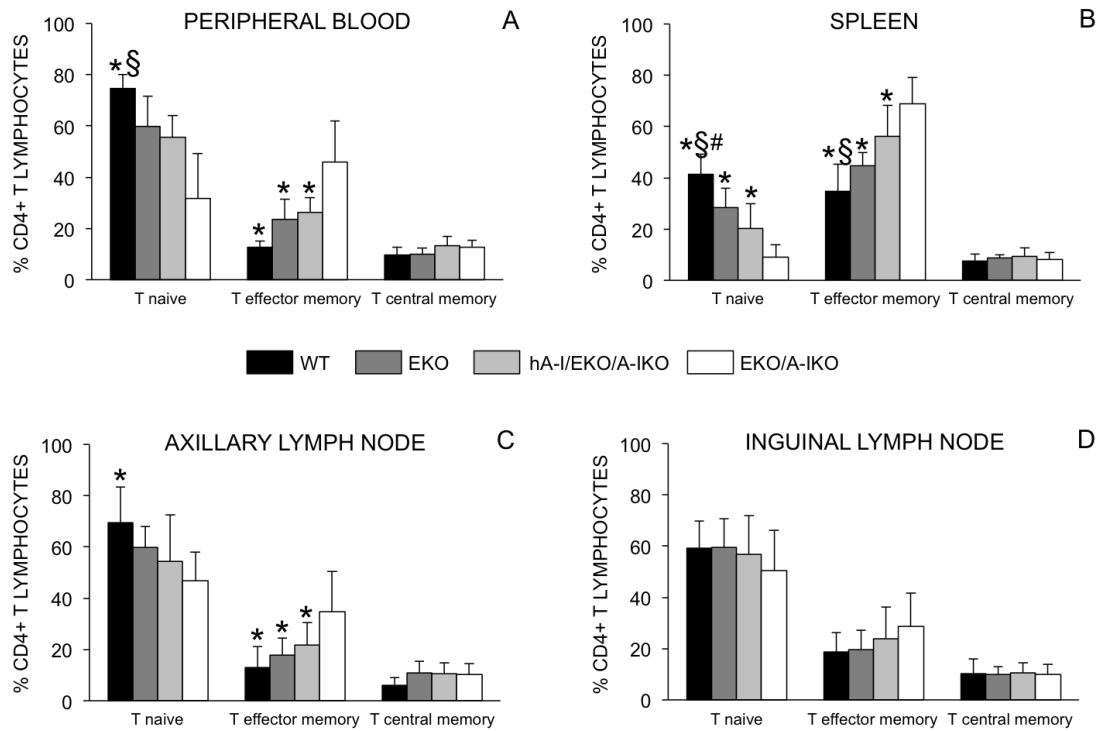


Figure 21. Percentage of CD4+ T lymphocytes in blood and lymphoid organs.

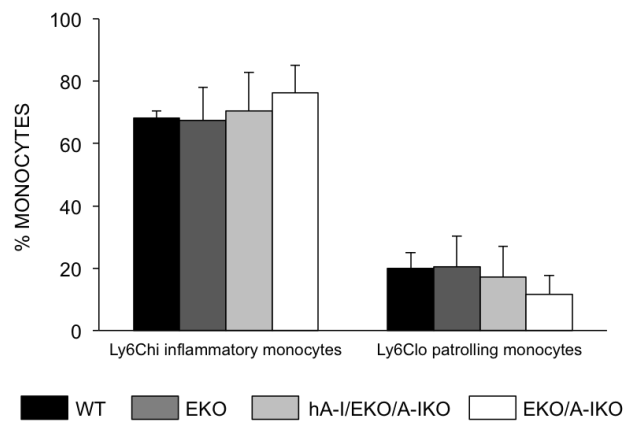


Figure 22. Percentage of monocytes.

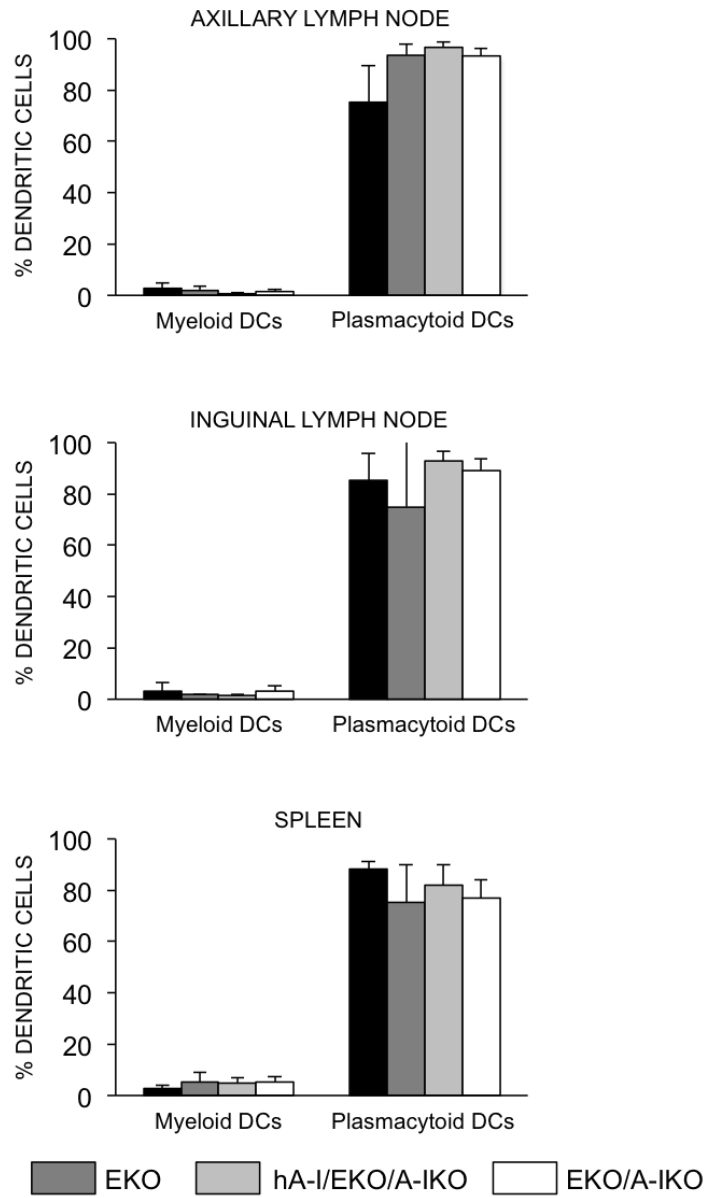


Figure 23. Percentage of dendritic cells in lymphoid organs.

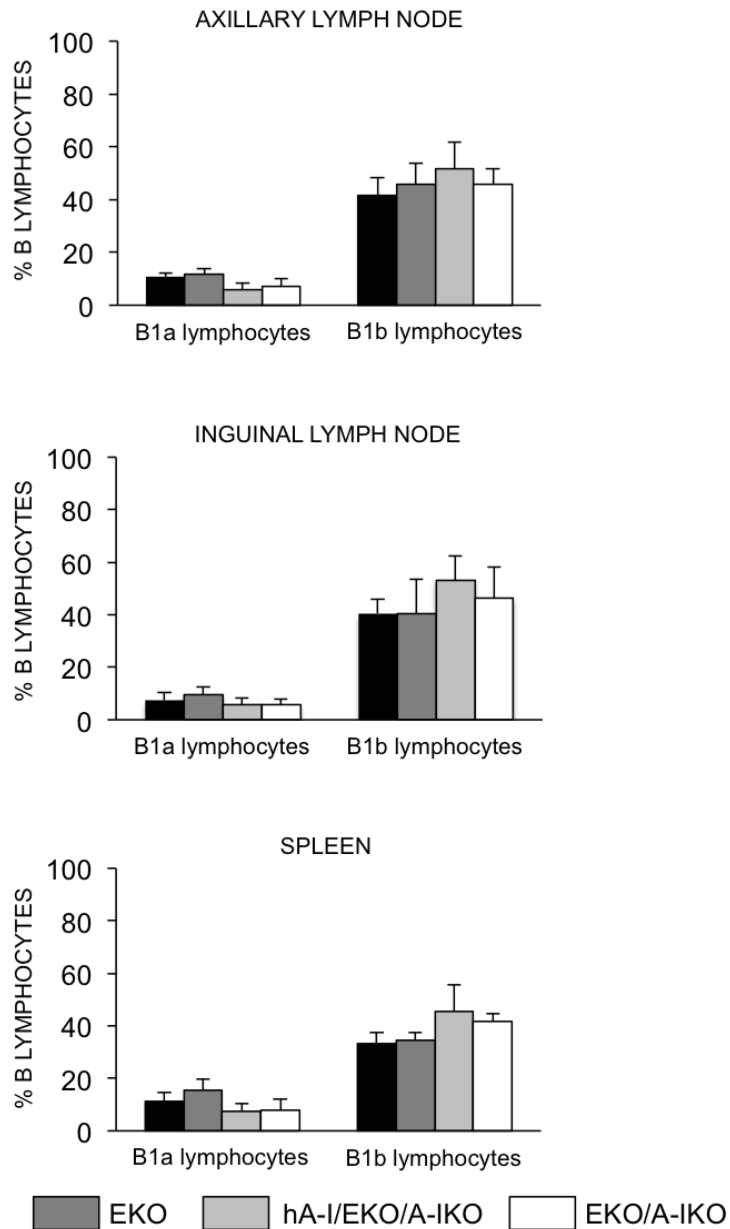


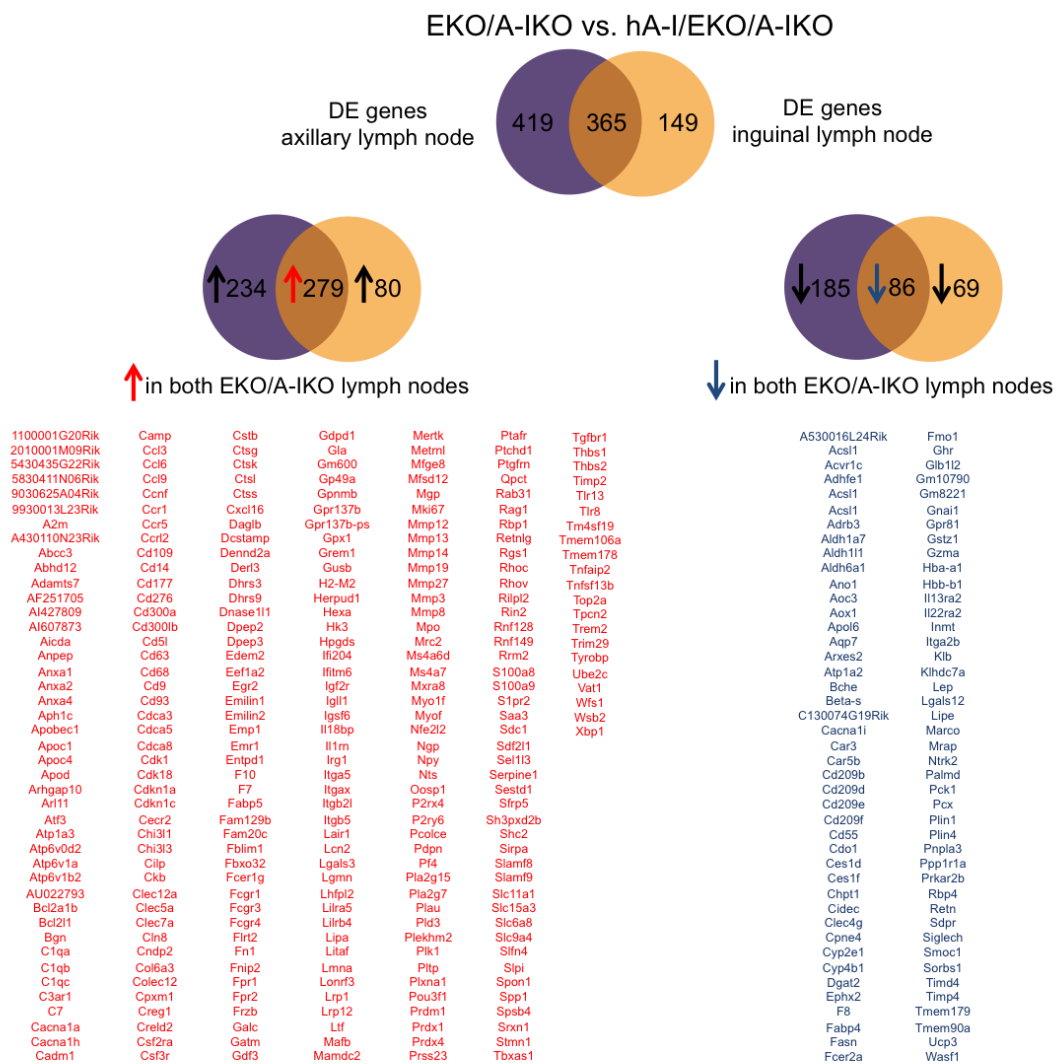
Figure 24. Percentage of B lymphocytes in lymphoid organs.

Secondary lymphoid organs transcriptomics

PolyA+ RNA recovered from axillary/inguinal lymph nodes and spleen of EKO/A-IKO and hA-I/EKO/A-IKO mice (representing the two extremes of apoA-I concentration) was subjected to sequencing on an Illumina HiSeq2000 instrument (3 biological replicates for each experimental condition). An average of 21×10^6 reads was produced by each sequencing reaction for each biological replicate, virtually all the reads passed the QF, of these, between 95% and 99% mapped consistently to the

reference transcriptome. Direct comparisons between the transcriptomes of the two different genotypes were performed.

In total, 784 genes were identified as differentially expressed (DE) in the axillary lymph node and 514 in the inguinal lymph node after comparing the two genotypes. Of them, 365 genes resulted DE in both lymph nodes (279 upregulated in EKO/A-IKO vs. hA-I/EKO/A-IKO mice and 86 downregulated in EKO/A-IKO vs. hA-I/EKO/A-IKO mice).



To better understand the biological significance of the data gathered from the transcriptome analysis, the Gene Ontology (GO) approach was used to perform an enrichment analysis on the gene sets. GO terms (GOterm Biological Process) upregulated in both axillary and inguinal lymph nodes of EKO/A-IKO vs. hA-I/EKO/A-IKO mice were related to immune response, response to wounding, inflammatory

response, chemotaxis, positive regulation of endocytosis, phagocytosis and proteolysis. Upregulated genes were mainly involved in lysosomal degradation (Cd63, Cd68, Ctsg, Ctsk, Ctsl, Ctss, Lipa, Slc11a1), cytokine-cytokine receptor interaction (Ccl3, Ccl6, Ccl9, Ccr1, Ccr5), cell adhesion (Cd276, Cadm1, H2-M2, Itgb2l), hematopoiesis (CD9, CD14), innate and adaptive immune response (Mpo, Clec7a, Fcer1g, Fcgr1, Fcgr3, Aicda, C1qc, C1qa, C1qb, Il18bp, Prdx1, Tlr8, Tlr13), and metalloprotease activity (Mmp3, Mmp8, Mmp12, Mmp13, Mmp14, Mmp19).

GO terms downregulated in both lymph nodes of EKO/A-IKO vs. hA-I/EKO/A-IKO mice were involved in fatty acid metabolism and oxidation/reduction.

In the spleen, the comparison of the transcriptomes obtained from EKO/A-IKO and hA-I/EKO/A-IKO mice showed substantially no differences with only six DE genes, downregulated in EKO/A-IKO mice (Apol11b, Cyr61, Dnaja1, Dnajb1, Hspa1a, Hspa1b, Hsph1).

DISCUSSION

Several studies have clearly established that HDL cholesterol levels are inversely associated with the incident of cardiovascular events (Gordon et al 1989). The major protective role exerted by HDLs is related to reverse cholesterol transport (RCT), a process that removes cholesterol from peripheral cells, including the vessel walls, and delivers it to the liver for excretion into the biliary system (Rosenson et al 2012). On the other hand, VLDL and LDL particles transport and deliver cholesterol to peripheral tissues, such as arteries, carrying out an atherogenic action. Recent studies have demonstrated that the HDL-induced athero-protection is also mediated by anti-oxidant, anti-apoptotic, anti-inflammatory and anti-thrombotic effects. The use of animal models has increased our understanding of atherosclerosis. Mouse represents the most frequently used species for study atherosclerotic process (Getz et al 2012). In particular, the EKO mouse is the most widely used model of atherosclerosis, characterized by the deletion of gene coding for the expression of apoE, the apolipoprotein which plays an important roles in lipoprotein metabolism. These mice, maintained at chow diet (low fat, no cholesterol) exhibit a strong hypercholesterolemia, condition associated with atherosclerosis development at the aortic sinus (Imazuimi et al 2011). Conversely, the murine model A-IKO, characterized by the deletion of apoA-I, the main protein component of HDL, shows a significant reduction of total cholesterol and plasma HDL, but this effect is not associated with an increase of atherosclerosis susceptibility (Li et al 1999).

The aim of the present project was to evaluate the effects of HDLs on atherosclerosis development, phenotype, inflammation and immune function through the use of genetically modified mice deprived of, or overexpressing, apoA-I, in the apoEKO background.

The first effect of the apoA-I deficiency was on plasma cholesterol levels and its distribution among lipoproteins. An increase would be expected in VLDL and LDL due to the deletion of apoE together with an almost total absence of HDLs, caused by the deletion of apoA-I. The results of the enzymatic assay for total cholesterol, both on plasma and lipoprotein fractions obtained by FPLC, have partially confirmed this expectation. EKO/A-IKO mice showed an increase in VLDL/LDL cholesterol and a severe decrease of HDL cholesterol. However, the cholesterolemia in EKO/A-IKO animals was comparable with that measured in C57BL/6 mice and was 3-fold lower than the concentration observed in EKO and hA-I/EKO/A-IKO mice. This latter mouse model, is characterized by a large HDL cholesterol peak and by a marked presence of VLDL-LDL particles, although less prominent than in EKO animals.

Despite a dramatic reduction in HDL levels, A-IKO mice did not show an increase in susceptibility to atherosclerosis development. The lack of atherosclerosis lesions in apoA-I deficient mice could be explained by the presence in this model of considerable amounts of apoE, which may functionally compensate, at least in part, for the apoA-I deficiency. Based on this experimental evidence and on the modest increase in circulating VLDLs and LDLs observed in EKO/A-IKO mice, no marked development of atherosclerotic lesions was expected in this model. En-face analysis of the aorta detected a comparable number of atherosclerotic plaques between EKO/A-IKO and EKO animals. Conversely, an unexpected result was instead obtained through histological evaluation with hematoxylin&eosin and Oil Red O staining of the cardiac district. Surprisingly, EKO/A-IKO mice not only developed atherosclerotic plaques at the aortic sinus, with a wider extension than the EKO animals, but also showed atherosclerotic lesions in the common coronary arteries. Previous studies performed on mice lacking both LDLR and apoA-I, fed high fat diet, displayed an atherosclerosis development at the aortic sinus with the same extent compared to single knockout LDLR mice (Zalabawi et al 2003). Standard murine models of atherosclerosis did not develop lesions in coronary artery. But genetic combination, obtained by crossing different knockout model, can lead to atherosclerotic plaques in coronary arteries. Mice deficient in both apoE and LDLR, fed atherogenic diet for 7 month, showed atherosclerosis in this district (Caligiuri et al 1999). The murine model EKO/SR-BIKO displayed coronary arterial lesion and premature death at 5 week of age (Braun et al 2002). The molecular mechanisms responsible for the larger extension of atherosclerotic plaques at the aortic sinus and the presence of atherosclerotic lesions in the common coronary arteries in EKO/A-IKO mice, may be due to an altered cholesterol flux into or out of the artery wall, and a decreased RCT. Both apoA-I and apoE play a central role in lipoprotein metabolism and can protect mice from atherosclerosis. ApoE influences atherosclerosis stimulating reverse cholesterol transport and activating enzymes involved in lipoprotein metabolism such as hepatic lipase HL, CETP and LCAT. This apolipoprotein also shows an important role in the clearance of atherogenic lipoproteins, in its absence cholesterol and triglyceride-rich lipoproteins accumulate in the blood resulting in increased of deposition in the vasculature (Mahley 1988). In addition, apoE exerts local effects of the artery, facilitating the efflux of cholesterol from the macrophages. Apo-I is directly involved in RCT preventing the accumulation of lipid in the vessel walls of arteries, mediating cholesterol efflux from cells and participating in clearance of lipoproteins from plasma. Our results suggest that EKO/A-IKO mice could be considered an innovative murine model of occlusive coronary artery disease useful to investigate

the mechanisms underlying the development of atherosclerosis and to study the role of endogenous factors or the effects of pharmacological therapies on coronary atherosclerosis.

Conversely, in hA-I/EKO/A-IKO animals, murine line characterized by high level of apoA-I, no atherosclerosis was observed in any of the segments of aorta and in the cardiac district. Therefore, these results support the concept that HDL apoA-I is highly protective against atherosclerosis. Previous studies have showed a direct antiatherogenic role for apoA-I, demonstrating that high level of apoA-I and HDL dramatically reduce atherogenesis (Badimon et al 1990) (Pászty et al 1994).

In addition to atherosclerosis development, we observed in EKO/A-IKO mouse an interesting cutaneous phenotype. In particular, this mouse model was characterized by deep alterations in the skin structure, with a massive dermal accumulation of cholesterol clefts, foam cells and T lymphocytes. Conversely, hA-I/EKO/A-IKO mice displayed a normal phenotype comparable with that of EKO and C57Bl/6 animals. Modifications of skin morphology have been reported in other genetically modified mouse models, all characterized by a severe, genetically- and/or dietary-induced, hypercholesterolemia. Particularly, skin abnormalities have been observed in hypercholesterolemic EKO mice and low-density lipoprotein receptor (LDLR) KO mice crossed with mice deficient in acyl-CoA acyltransferase-1 (ACAT1), the enzyme that catalyzes intracellular cholesterol esterification (Accad et al 2000). These mice showed hair loss, xanthomatosis, and marked thickening of the dermis with diffuse extracellular cholesterol crystals, accompanied by a severe inflammatory cell infiltrate. Severe xanthomatosis and foam cell accumulation was also observed in EKO mice with macrophage inactivation of ABCA1 (Aiello et al 2002); Finally, in hypercholesterolemic LDLRKO mice fed a high-fat/high-cholesterol diet, apoA-I deletion led to massive cholesterol accumulation in skin, accompanied by an increase in dermal thickness, hair loss and macrophage infiltration (Zabalawi et al 2007)(Wilhelm et al 2010). The present study shows that hyperlipidemia is not an essential requirement for the development of skin abnormalities, but that HDL deficiency itself can drive a massive dermal lipid deposition in mice, in the presence of normal plasma cholesterol levels. Xanthomas arising from this specific dyslipidemic condition have been poorly analyzed in humans. One case report, showing the histological features of xanthomas arising from an HDL deficiency status, documented the presence of T lymphocytes, as well as of clusters of foam cells with free and esterified cholesterol accumulation (Lindeskog et al 1972). These features resemble those found in our study in EKO/A-IKO mice, thus suggesting that this genetically modified mouse line could represent a valid animal

model for the study of this pathological skin condition. The deletion of both apoA-I and apoE led to the formation of macrophage-derived foam cells able to accumulate esterified cholesterol in their cytoplasm. Since in this mouse model cholesterol efflux is impaired, toxic free cholesterol possibly accumulates causing cell death and, as a consequence, dermal deposition of cholesterol clefts which possibly results in an inflammatory condition. This model reproduces for the first time the cutaneous phenotype of human apoA-I deficiency, characterized by xanthomatous deposition in the absence of a hyperlipidemic status. This experimental model will thus represent a useful tool for investigating, through time course studies, the onset and mechanisms involved in the development of this cutaneous pathological condition.

The present work also demonstrated that the deficiency of apoA-I in apoEKO background lead to an enlargement of skin draining lymph nodes characterized by foamy macrophages accumulation and cholesterol deposition, predisposing to granulomatous reactions. Previous studies on mice lacking LDLR and apoA-I genes, displayed enlargement and inflammation in the lymph nodes in response to an atherogenic diet (Wilhelm et al 2009). In contrast, hA-I/EKO/A-IKO and EKO mice did not show an increase in lymph nodes size or cellularity. These results suggest that plasma apoA-I prevents lymph node enlargement, lipid accumulation and peripheral lymphocytes proliferation. Cholesterol accumulation in skin draining lymph nodes could be explained by the impaired cholesterol efflux. The combined analysis of lymph nodes transcriptome revealed that apoA-I deficiency in apoEKO background cause a widespread induction of gene related to innate and adaptive immune responses, particularly those associated to lysosomal activity in phagocytes as well as to T-lymphocyte and B-lymphocyte activation.

In parallel we also characterized mouse leukocytes by flow cytometry. In peripheral blood and lymphoid organs EKO/A-IKO mice displayed a significant increase in the percentage of CD4⁺ T effector memory lymphocytes compared to the other murine lines. This subset of CD4⁺ is strongly associated with atherosclerosis supporting the relevance of adaptive response in cardiovascular disease (Lahoute et al 2011). Lymph nodes immune cells are involved in atherosclerosis from the formation of foam cells to the migration of dendritic cells from atherosclerotic lesions to lymph nodes. CD4⁺ effector memory cells are supposed to migrate into atherosclerotic plaques where they sustain the inflammatory response (Ammirati et al 2012). Thus, the marked atherosclerosis in EKO/A-IKO mice could also be explained, at least in part, by a modulation of the inflammatory response mediated by CD4⁺ T lymphocytes. Interestingly, the presence of plasma apoA-I increased

T naïve cells and decrease T effector memory cells suggesting that this apolipoprotein can control T cell homeostasis in peripheral blood and lymph nodes by regulating the T naïve/T effector balance.

In conclusion, the present study demonstrated that apoA-I deficiency in apoEKO background brings about severe atherosclerosis at the aortic sinus. Surprisingly, this model show atherosclerotic plaques also at common coronary arteries, thus may prove to be a useful model to investigate the mechanisms underlying the development of coronary disease. The experiments described in the present work helped in clarifying the role of apoA-I in inflammation. The deletion of apoA-I in athero-prone murine line lead to cholesterol accumulation and inflammation in skin and skin draining lymph nodes. These results are also associated with activation and increase in CD4+ T effector memory lymphocytes in peripheral blood and lymphoid organs. These effects were obtained, for the first time, with low plasma cholesterol levels and without dietary challenge, but only with genotype influence. Taken together our results suggest a strong association between plasma apoA-I, cholesterol metabolism, atherosclerosis, inflammation and autoimmunity.

REFERENCES

- Abumrad** NA et al. Role of the gut in lipid homeostasis. *Physiol Rev.* 2012 Jul;92(3):1061-85.
- Accad** M et al. Massive xanthomatosis and altered composition of atherosclerotic lesions in hyperlipidemic mice lacking acyl CoA:cholesterol acyltransferase 1. *J Clin Invest.* 2000; 105: 711-9.
- Aiello** RJ et al. Increased atherosclerosis in hyperlipidemic mice with inactivation of ABCA1 in macrophages. *Arterioscler Thromb Vasc Biol.* 2002; 22: 630-7.
- Alphonse** PA et al. Revisiting Human Cholesterol Synthesis and Absorption: The Reciprocity Paradigm and its Key Regulators. *Lipids.* 2016 May;51(5):519-36.
- Altmann** SW et al. Niemann-Pick C1 Like 1 protein is critical for intestinal cholesterol absorption. *Science.* 2004 Feb 20;303(5661):1201-4.
- Ammirati** E et al Effector memory T cells are associated with atherosclerosis in humans and animal models. *J Am Heart Assoc.* 2012; 1(1):27-41.
- Badimon** J et al. Regression of atherosclerotic lesions by high density lipoprotein fraction in the cholesterol-fed rabbit. *J. Clin. Invest.* 1990; 85:1234-1241.
- Bandeali** S et al High-density lipoprotein and atherosclerosis: the role of antioxidant activity. *Curr Atheroscler Rep.* 2012 Apr;14(2):101-7.
- Baker** PW, et al. Ability of reconstituted high density lipoproteins to inhibit cytokine-induced expression of vascular cell adhesion molecule-1 in human umbilical vein endothelial cells. *J Lipid Res.* 1999;40(2):345-53.
- Besler** C et al Mechanisms underlying adverse effects of HDL oneNOS-activating pathways in patients with coronary artery disease. *Journal of Clinical Investigation.* 2011;121:2693-2708.
- Bastiaanse** L et al. The effect of membrane cholesterol content on ion transport processes in plasma membranes. *Cardiovascular Research.* 1997; 33:272-283.
- Beutler** B et al. How we detect microbes and respond to them: the Toll-like receptors and their transducers. *J. Leukoc. Biol.* 2003. 74: 479-485.
- Borgstrom** BJ et al. Studies on intestinal cholesterol absorption in the human. *Clin Invest.* 1960 Jun;39:809-15.
- Braun** A et al. Loss of SR-BI expression leads to the early onset of occlusive atherosclerotic coronary artery disease, spontaneous myocardial infarctions, severe cardiac dysfunction, and premature death in apolipoprotein E-deficient mice. *Circ Res.* 2002 Feb 22;90(3):270-6.

- Brooks-Wilson** A et al. Mutations in ABC1 in Tangier disease and familial high-density lipoprotein deficiency. *Nat Genet.* 1999 Aug;22(4):336-45.
- Broos** K et al. Platelets at work in primary hemostasis. *Blood Rev* 2011;25:155–167.
- Brown** MS et al. The SREBP pathway: regulation of cholesterol metabolism by proteolysis of a membrane-bound transcription factor. *Cell.* 1997 May 2;89(3):331-40.
- Brunham** LR et al. Intestinal ABCA1 directly contributes to HDL biogenesis in vivo. *J Clin Invest.* 2006 Apr;116(4):1052-62.
- Calabresi** L et al Inhibition of VCAM-1 expression in endothelial cells by reconstituted high density lipoproteins. *Biochem Biophys Res Commun.*1997 Sep 8;238(1):61-5.
- Calabresi** L et al. Endothelial protection by highdensity lipoproteins: from bench to bedside. *Arterioscler. Thromb. Vasc. Biol.* 2003;23, 1724-1731.
- Caligiuri** G et al. Myocardial infarction mediated by endothelin receptor signaling in hypercholesterolemic mice.*Proc Natl Acad Sci U S A.*1999;96:6920–6924.
- Calkin** AC et al Reconstituted high-density lipoprotein attenuates platelet function in individuals with type 2 diabetes mellitus by promoting cholesterol efflux. *Circulation.*2009 Nov 24;120(21):2095-104.
- Charlton-Menys** V. et al. Human cholesterol metabolism and therapeutic molecules. *Exp Physiol.* 2008 Jan;93(1):27-42.
- Chau** P et al Bone morphogenetic protein-1 (BMP-1) cleaves human proapolipoprotein A1 and regulates its activation for lipid binding. *Biochemistry.*2007 Jul 17;46(28):8445-50.
- Christoffersen** C et al Endothelium-protective sphingosine-1-phosphate provided by HDL-associated apolipoprotein M. *Proc. Natl.Acad. Sci. U. S. A.* 2001;108, 9613-9618.
- Cockerill** GW et al. High-density lipoproteins inhibit cytokine-induced expression of endothelial cell adhesion molecules. *Arterioscler Thromb Vasc Biol.* 1995 Nov;15(11):1987-94.
- Coleman** R et al A mouse model for human atherosclerosis: long-term histopathological study of lesion development in the aortic arch of apolipoprotein E-deficient (E0) mice. *Acta Histochem.*2006;108(6):415-24.
- Cooper** AD et al. Hepatic uptake of chylomicron remnants. *J Lipid Res.* 1997 Nov;38(11):2173-92.
- Corash** L et al Regulation of thrombopoiesis: effects of the degree of thrombocytopenia on megakaryocyte ploidy and platelet volume. *Blood* 1987;70:177–185.

- Davidson** MH et al Update on CETP inhibition. *J Clin Lipidol*. 2010 Sep-Oct;4(5):394-8.
- Di Angelantonio** E et al Major lipids, apolipoproteins, and risk of vascular disease. *Journal of the American Medical Association* 2009; 302:1993–2000.
- Döring** Y et al Auto-antigenic protein-DNA complexes stimulate plasmacytoid dendritic cells to promote atherosclerosis. *Circulation*.2012 Apr 3;125(13):1673-83.
- Driscoll** DM et al. Molecular and cell biology of lipoprotein biosynthesis. *Methods Enzymol*.1986;128:41-70.
- Duan** P et al. Cholesterol absorption is mainly regulated by the jejunal and ileal ATP-binding cassette sterol efflux transporters Abcg5 and Abcg8 in mice. *J. Lipid Res*. 2004; 45:1312–2.
- Duewell** P et al. Nlrp3 inflammasomes are required for atherogenesis and activated by cholesterol crystals. *Nature*. 2010; 464:1357–1361.
- Duong** PT et al Characterization and properties of pre beta-HDL particles formed by ABCA1-mediated cellular lipid efflux to apoA-I. *J Lipid Res*. 2008 May;49(5):1006-14.
- Epanand** RM et al HDL and apolipoprotein A-I protect erythrocytes against the generation of procoagulant activity. *Arterioscler Thromb*.1994 Nov;14(11):1775-83.
- Falk** E et al Update on acute coronary syndromes: the pathologists' view. *Eur Heart J*. 2013; 34:719–728.
- Farb** A et al. Coronary plaque erosion without rupture into a lipid core. A frequent cause of coronary thrombosis in sudden coronary death. *Circulation*. 1996; 93:1354– 1363.
- Favari** E et al Small discoidal pre-beta1 HDL particles are efficient acceptors of cell cholesterol via ABCA1 and ABCG1. *Biochemistry*. 2009 Nov 24;48(46):11067-74.
- Folch** J et al. A simple method for the isolation and purification of total lipides from animal tissues. *J Biol Chem*. 1957; 226: 497-509.
- Franceschini** G et al Reverse cholesterol transport: physiology and pharmacology. *Atherosclerosis*. 1991 Jun;88(2-3):99-107.
- Fuller** M et al The effects of diet on occlusive coronary artery atherosclerosis and myocardial infarction in scavenger receptor class B, type 1/low-density lipoprotein receptor double knockout mice.*Arterioscler Thromb Vasc Biol*.2014 Nov;34(11):2394-403.
- Galkina** E et al. Immune and inflammatory mechanisms of atherosclerosis. *Annu Rev Immunol*.2009;27:165-97.

Garner B et al Oxidation of high density lipoproteins. II. Evidence for direct reduction of lipid hydroperoxides by methionine residues of apolipoproteins AI and AII. *J Biol Chem.* 1998;273:6088-6095.

Getz GS et al. Animal models of atherosclerosis. *Arterioscler Thromb Vasc Biol.*2012 May;32(5):1104-15.

Gimbrone MA et al. Endothelial dysfunction, hemodynamic forces, and atherogenesis. *Ann N Y Acad Sci.*2000 May;902:230-9.

Glass C et al. Dissociation of tissue uptake of cholesterol ester from that of apoprotein A-I of rat plasma high density lipoprotein: selective delivery of cholesterol ester to liver, adrenal, and gonad. *Proc Natl Acad Sci U S A.*1983 Sep;80(17):5435-9.

Goedeke L et al. Regulation of cholesterol homeostasis. *Cell Mol Life Sci.* 2012 Mar;69(6):915-30.

Goldstein JL et al. Receptor-mediated endocytosis: concepts emerging from the LDL receptorsystem. *Annu Rev Cell Biol.*1985;1:1-39.

Goldstein JL et al. Regulation of the mevalonate pathway. *Nature.* 1990; 343:425–430.

Goldstein JL et al. The LDL receptor. *Arterioscler Thromb Vasc Biol.* 2009 Apr;29(4):431-8.

Gordon T et al High density lipoprotein as a protective factor against coronary heart disease. The Framingham Study. *Am J Med.* 1977 May;62(5):707-14.

Gordon DJ et al High-density lipoprotein--the clinical implications of recent studies. *N Engl J Med.* 1989 Nov 9;321(19):1311-6.

Greenow K et al The key role of apolipoprotein E in atherosclerosis. *J Mol Med (Berl).*2005 May;83(5):329-42.

Griffin J et al. Plasma lipoproteins, hemostasis and thrombosis. *Thromb Haemost.* 2001;86:386–394.

Grundy SM. et al. Cholesterol metabolism in man. *West J Med.* 1978 Jan;128(1):13-25.

Gu F et al. Structures of discoidal high density lipoproteins: a combined computational-experimental approach. *J Biol Chem.* 2010 Feb 12;285(7):4652-65.

Hamilton R.L. et al- Synthesis and secretion of plasma lipoproteins. *Adv.Exp. Med.Biol.*1972; 26:7–24.

- Hajduk** SL et al Lysis of *Trypanosoma brucei* by a toxic subspecies of human high density lipoprotein. *J Biol Chem*. 1989;264:5210-5217.
- Hansson** GK The B cell: a good guy in vascular disease? *Arterioscler Thromb Vasc Biol*. 2002 Apr 1;22(4):523-4.
- Hansson** GK et al Inflammation and atherosclerosis. *Annu Rev Pathol*. 2006;1:297-329.
- Hartvigsen** K et al. A diet-induced hypercholesterolemic murine model to study atherogenesis without obesity and metabolic syndrome. *Arterioscler Thromb Vasc Biol*. 2007; 27:878-885.
- Hauser** H et al. Identification of a receptor mediating absorption of dietary cholesterol in the intestine. *Biochemistry*. 1998 Dec 22;37(51):17843-50.
- Hofker** MH et al Transgenic mouse models to study the role of APOE in hyperlipidemia and atherosclerosis. *Atherosclerosis*. 1998 Mar;137(1):1-11.
- Hoofnagle** AN et al. Lipoproteomics: using mass spectrometry based proteomics to explore the assembly, structure, and function of lipoproteins *J Lipid Res*. 2009 Oct;50(10):1967-75.
- Horton** JD et al. SREBPs: activators of the complete program of cholesterol and fatty acid synthesis in the liver. *J Clin Invest*. 2002 May;109(9):1125-31.
- Hussain** MM et al. Chylomicron assembly and catabolism: role of apolipoproteins and receptors. *Biochim Biophys Acta*. 1996 May 20;1300(3):151-70.
- Hussain** M et al. A proposed model for the assembly of chylomicrons. *Atherosclerosis*. 2000; 148:1-15.
- Imaizumi** K et al. Diet and atherosclerosis in apolipoprotein E-deficient mice. *Biosci Biotechnol Biochem*. 2011;75(6):1023-35.
- Ikonen** E. et al Cellular cholesterol trafficking and compartmentalization. *Nat. Rev. Mol. Cell Biol*. 2008; 9:125 – 138.
- Jessup** W et al. Roles of ATP binding cassette transporters A1 and G1, scavenger receptor BI and membrane lipid domains in cholesterol export from macrophages. *Curr Opin Lipidol*. 2006; 17: 247-57.
- Ji** A et al. Scavenger receptor SR-BI in macrophage lipid metabolism. *Atherosclerosis*. 2011 Jul;217(1):106-12.
- Jonasson** L et al Regional accumulations of T cells, macrophages, and smooth muscle cells in the human atherosclerotic plaque. *Arteriosclerosis*. 1986 Mar-Apr;6(2):131-8.

Julve J et al. Chylomicrons: Advances in biology, pathology, laboratory testing, and therapeutics. *Clin Chim Acta*. 2016 Apr 1;455:134-48.

Kaul S et al: Rapid reversal of endothelial dysfunction in hypercholesterolemic apolipoprotein E-null mice by recombinant apolipoprotein AI(Milano)-phospholipid complex. *J. Am. Coll. Cardiol*. 2004; 44:1311-1319.

Kellner-Weibel G et al Effects of intracellular free cholesterol accumulation on macrophage viability: a model for foam cell death. *Arterioscler Thromb Vasc Biol*. 1998 Mar;18(3):423-31.

Khovidhunkit W et al. Effects of infection and inflammation on lipid and lipoprotein metabolism: mechanisms and consequences to the host. *J. Lipid Res*. 2004;45: 1169–1196.

Krauss RM et al Lipoprotein subfractions and cardiovascular disease risk. *Curr Opin Lipidol*.2010 Aug;21(4):305-11.

Kumar NS et al. Prechylomicron transport vesicle: isolation and partial characterization. *Am.J.Physiol*. 1999;276:378–386.

Kuvin JT et al A novel mechanism for the beneficial vascular effects of high-density lipoprotein cholesterol: enhanced vasorelaxation and increased endothelial nitric oxide synthase expression. *Am. Heart J*. 2002;144:165-172.

Lahoute C et al Adaptive immunity in atherosclerosis: mechanisms and future therapeutic targets. *Nat Rev Cardiol*.2011 Jun;8(6):348-58.

Lambert G et al Hepatic lipase promotes the selective uptake of high density lipoprotein-cholesteryl esters via the scavenger receptor B1. *J Lipid Res*.1999 Jul;40(7):1294-303.

Lee RG et al. Differential expression of ACAT1 and ACAT2 among cells within liver, intestine, kidney, and adrenal of nonhuman primates. *J. Lipid Res*. 2000; 41:1991–2001.

Levy E et al. Intestinal cholesterol transport proteins: an update and beyond. *Curr Opin Lipidol*. 2007 Jun;18(3):310-8.

Li D et al Inhibition of arterial thrombus formation by ApoA1 Milano. *Arterioscler Thromb Vasc Biol*.1999 Feb;19(2):378-83.

Li H et al Lack of ApoA-I Is Not Associated With Increased Susceptibility to Atherosclerosis in Mice. *Arterioscler Thromb Vasc Biol*. 1993;13:1814-1821.

Libby P et al. Interleukin-1: a mitogen for human vascular smooth muscle cells that induces the release of growth-inhibitory prostanoids. *J Clin Invest.* 1988; 81:487–498.

Libby P. Changing concepts of atherogenesis. *J Intern Med.* 2000;247:349-358.

Libby P Inflammation and atherosclerosis. *Circulation.* 2002 Mar 5;105(9):1135-43.

Libby P et al. Inflammation and its resolution as determinants of acute coronary syndromes. *Circ Res.* 2014; 114:1867–1879.

Lindeskog GR et al. Serum lipoprotein deficiency in diffuse "normolipemic" plane xanthoma. *Arch Dermatol.* 1972; 106:529-32.

Mahley R Apolipoprotein E: cholesterol transport protein with expanding role in biology. *Science.* 1988; 240:622-630.

Martin JF et al. The causal role of megakaryocyte-platelet hyperactivity in acute coronary syndromes. *Nat Rev Cardiol.* 2012;9:658–670.

Meaney S et al. Epigenetic regulation of cholesterol homeostasis. *Front Genet.* 2014 Sep 24;5:311.

Miller NE. Raising high density lipoprotein cholesterol. The biochemical pharmacology of reversecholesterol transport. *Biochem Pharmacol.* 1990 Aug 1;40(3):403-10.

Mjos OD et al. Characterization of remnants produced during the metabolism of triglyceride rich lipoproteins of blood plasma and intestinal lymph in the rat. *J Clin Invest.* 1975 Sep;56(3):603-15.

Myant N.B. The biology of cholesterol and related steroids. *Medical Books Ltd.* London 1981.

Nakamura K et al. Expression and regulation of multiple murine ATP-binding cassette transporterG1 mRNAs/isoforms that stimulate cellular cholesterol efflux to high density lipoprotein. *J. Biol. Chem.* 2004; 279(44):45980–89.

Nakashima Y et al ApoE-deficient mice develop lesions of all phases of atherosclerosis throughout the arterial tree. *Arterioscler Thromb.* 1994 Jan;14(1):133-40.

Naqvi TZ et al Evidence that high-density lipoprotein cholesterol is an independent predictor of acute platelet-dependent thrombus formation. *Am J Cardiol.* 1999 Nov 1;84(9):1011-7.

Navab M et al. Monocyte transmigration induced by modification of low density lipoprotein in cocultures of human aortic wall cells is due to induction of monocyte chemotactic protein 1 synthesis and is abolished by high density lipoprotein. *J Clin Invest.* 1991 Dec;88(6):2039-46.

Navab M et al. Normal high density lipoprotein inhibits three steps in the formation of mildly oxidized low density lipoprotein: Steps 2 and 3. *J. Lipid Res.* 2000;41:1495-1508.

Navab M et al HDL and the inflammatory response induced by LDL-derived oxidized phospholipids. *Arterioscler Thromb Vasc Biol.* 2001 Apr;21(4):481-8.

Navab M et al. HDL and cardiovascular disease: atherogenic and atheroprotective mechanisms. *Nature Reviews Cardiology.* 2011; 8:222-232.

Nichols AV et al. Nondenaturing polyacrylamide gradient gel electrophoresis. *Methods Enzymol.* 1986; 128: 417-31.

Nofer JR et al. High density lipoproteins enhance the Na⁺/H⁺ antiport in human platelets. *Thromb Haemost.* 1996 Apr;75(4):635-41.

Nofer JR et al Suppression of endothelial cell apoptosis by high density lipoproteins (HDL) and HDL-associated lysosphingolipids. *J Biol Chem.* 2001 Sep 14;276(37):34480-5.

Olofsson SO et al. Intracellular assembly of VLDL: two major steps in separate cell compartments. *Trends Cardiovasc Med.* 2000 Nov;10(8):338-45.

Out R et al. Combined deletion of macrophage ABCA1 and ABCG1 leads to massive lipid accumulation in tissue macrophages and distinct atherosclerosis at relatively low plasma cholesterol levels. *Arterioscler. Thromb. Vasc. Biol.* 2008;28:258-64.

Pászty C et al Apolipoprotein AI transgene corrects apolipoprotein E deficiency-induced atherosclerosis in mice. *J Clin Invest.* 1994 Aug;94(2):899-903.

Pathansali R et al. Altered megakaryocyte-platelet haemostatic axis in hypercholesterolaemia. *Platelets.* 2001;12:292-297.

Peet DJ et al The LXRs: a new class of oxysterol receptors. *Curr Opin Genet Dev* 1998; 8(5):571-575.

Peet DJ et al. Cholesterol and bile acid metabolism are impaired in mice lacking the nuclear oxysterol receptor LXR alpha. *Cell.* 1998; 93(5):693-704.

Plump AS et al. Severe hypercholesterolemia and atherosclerosis in apolipoprotein E- deficient mice created by homologous recombination in ES cells. *Cell.* 1992;71(2):343-353.

Plump AS et al Human apolipoprotein A-I gene expression increases high density lipoprotein and suppresses atherosclerosis in the apolipoprotein E-deficient mouse. *Proc Natl Acad Sci U S A*.1994 Sep 27;91(20):9607-11.

Pomerantz KB et al. Enrichment of endothelial cell arachidonate by lipid transfer from high density lipoproteins: relationship to prostaglandin I₂ synthesis. *J. Lipid Res*. 1985; 26:1269-1276.

Rader DJ et al. Disorders of Lipoprotein Metabolism. In *Harrison's Principles of Internal Medicine*. 2008 2416–2429.

Randolph GJ Mechanisms that regulate macrophage burden in atherosclerosis.*Circulation Research*.2014;114(11):1757–1771.

Reizis B et al. Plasmacytoid dendritic cells: recent progress and open questions. *Annu Rev Immunol*.2011;29:163-83.

Riwanto M et al Altered activation of endothelial anti- and proapoptotic pathways by high-density lipoprotein from patients with coronary artery disease: role of high-density lipoprotein-proteome remodeling *Circulation*. 2013;127:891-904.

Roger VL et al Heart disease and stroke statistics 2012 update: a report from the American Heart Association. *Circulation*.2012 Jan 3;125(1):203-220.

Rosenfeld ME et al Inflammation and atherosclerosis: direct versus indirect mechanisms. *Curr Opin Pharmacol*.2013 Apr;13(2):154-60.

Rosenson RS et al. Effects of lipids and lipoproteins on thrombosis and rheology. *Atherosclerosis*. 1998;140:271–280.

Rosenson RS et al. Cholesterol efflux and atheroprotection: advancing the concept of reverse cholesterol transport. *Circulation*.2012 Apr 17;125(15):1905-19.

Rothblat GH et al Apolipoproteins, membrane cholesterol domains, and the regulation of cholesterol efflux. *J Lipid Res*. 1992 Aug;33(8):1091-7.

Rubin EM et al Inhibition of early atherogenesis in transgenic mice by human apolipoprotein AI. *Nature*1991 Sep 19;353(6341):265-7.

Sato K et al. Role of sphingosine 1-phosphate in anti-atherogenic actions of high-density lipoprotein. *World Journal of Biological Chemistry*. 2010;1:327–337.

Seimon T et al. Mechanisms and consequences of macrophage apoptosis in atherosclerosis. *Journal of Lipid Research*. 2009;50:382–387.

Shah AS et al. Proteomic diversity of high density lipoproteins: our emerging understanding of its importance in lipid transport and beyond. *J Lipid Res*. 2013;54:2575-2585.

Shelness GS et al. Very-low-density lipoprotein assembly and secretion. *Curr Opin Lipidol*. 2001 Apr;12(2):151-7.

Spieker LE et al: High-density lipoprotein restores endothelial function in hypercholesterolemic men. *Circulation*. 2002;105, 1399-1402.

Steinberg D Low density lipoprotein oxidation and its pathobiological significance. *J Biol Chem*. 1997 Aug 22;272(34):20963-6.

Suc I et al HDL and ApoA prevent cell death of endothelial cells induced by oxidized LDL. *Arterioscler Thromb Vasc Biol*. 1997 Oct;17(10):2158-66.

Sulpice JC et al Requirement for phosphatidylinositol 4,5-bisphosphate in the Ca(2+)-induced phospholipid redistribution in the human erythrocyte membrane. *J Biol Chem*. 1994 Mar 4;269(9):6347-54.

Sukhova G et al. Expression of the elastolytic cathepsins s and k in human atheroma and regulation of their production in smooth muscle cells. *J Clin Invest*. 1998; 102:576–583.

Suzuki H et al. A role for macrophage scavenger receptors in atherosclerosis and susceptibility to infection. *Nature*. 1997 Mar 20;386(6622):292-6.

Tamagaki T et al: Effects of high-density lipoproteins on intracellular pH and proliferation of human vascular endothelial cells. *Atherosclerosis*. 1996;123, 73-82.

Tatami R et al Intermediate-density lipoprotein and cholesterol-rich very low density lipoprotein in angiographically determined coronary artery disease. *Circulation*. 1981 Dec;64(6):1174-84.

Tiwari S. et al Intracellular trafficking and secretion of VLDL. *Arterioscler Thromb Vasc Biol*. 2012 May;32(5):1079-86.

Tward A et al Decreased atherosclerotic lesion formation in human serum paraoxonase transgenic mice. *Circulation*. 2002;106:484-490.

van der Wal AC et al. Site of intimal rupture or erosion of thrombosed coronary atherosclerotic plaques is characterized by an inflammatory process irrespective of the dominant plaque morphology. *Circulation*. 1994; 89:36–44.

Van Sickle WA et al. High density lipoprotein-induced cardiac prostacyclin synthesis in vitro: relationship to cardiac arachidonate mobilization. *J. Lipid Res.* 1986;27, 517-522.

Virmani R et al. Vulnerable plaque: the pathology of unstable coronary lesions. *J Interv Cardiol.* 2002;15:439-446.

von Eckardstein A et al. High density lipoproteins and arteriosclerosis. Role of cholesterol efflux and reverse cholesterol transport. *Arterioscler Thromb Vasc Biol.* 2001 Jan;21(1):13-27.

Wang DQ et al. Regulation of intestinal cholesterol absorption. *Annu.Rev.Physiol.*2007;69:221-48.

Wang LJ et al. Niemann-Pick C1-Like 1 and cholesterol uptake. *Biochim Biophys Acta.* 2012 Jul;1821(7):964-72.

WHO. Global status report on non communicable disease 2010. WHO press, World Health Organisation, 20 Avenue Appia, 1211 Geneva 27, Switzerland 2011.

Wilhelm AJ et al Apolipoprotein A-I and its role in lymphocyte cholesterol homeostasis and autoimmunity. *Arterioscler Thromb Vasc Biol.*2009 Jun;29(6):843-9.

Wilhelm AJ et al. Apolipoprotein A-I modulates regulatory T cells in autoimmune LDLr^{-/-}, ApoA-I^{-/-} mice. *J Biol Chem.*2010; 285: 36158-69.

Xia P et al High density lipoproteins (HDL) interrupt the sphingosine kinase signaling pathway. A possible mechanism for protection against atherosclerosis by HDL. *J Biol Chem.* 1999 Nov 12;274(46):33143-7.

Ye J et al. Regulation of cholesterol and fatty acid synthesis *Cold Spring Harb Perspect Biol.* 2011 Jul 1;3(7).

Yvan-Charvet L et al ATP-binding cassette transporters and HDL suppress hematopoietic stem cell proliferation. *Science.*2010 Jun 25;328(5986):1689-93.

Zabalawi M et al. Induction of fatal inflammation in LDL receptor and ApoA-I double-knockout mice fed dietary fat and cholesterol. *Am J Pathol.*2003 Sep;163(3):1201-13.

Zabalawi M et al. *J Lipid Res.* Inflammation and skin cholesterol in LDLr^{-/-}, apoA-I^{-/-} mice: link between cholesterol homeostasis and self-tolerance? 2007; 48: 52-65.

Zardi EM et al. Subclinical carotid atherosclerosis in elderly patients with primary Sjögren syndrome: a duplex Doppler sonographic study. *Int J Immunopathol Pharmacol.*2014;27:645–651.

Zhang SH, et al. Spontaneous hypercholesterolemia and arterial lesions in mice lacking apolipoprotein E. *Science*. 1992; 258(5081):468–471.

Zhang X et al Endothelium-dependent and independent functions are impaired in patients with coronary heart disease. *Atherosclerosis*. 2000; 149:19-24.